(NASA-CR-186337) NASA 60 GHz INTERSATELLITE COMMUNICATION LINK DEFINITION STUDY. ADDENDUM A: MIXED BASEBAND AND IF SIGNALS (Ford Aerospace and Communications Corp.) 69 p

N90-23593

Unclas
CSCL 17B G3/32 0264891

Addendum A to

NASA 60 GHz Intersatellite Communication Link Definition Study

Modification of Contract NAS5-28589

Mixed Baseband and IF Signals

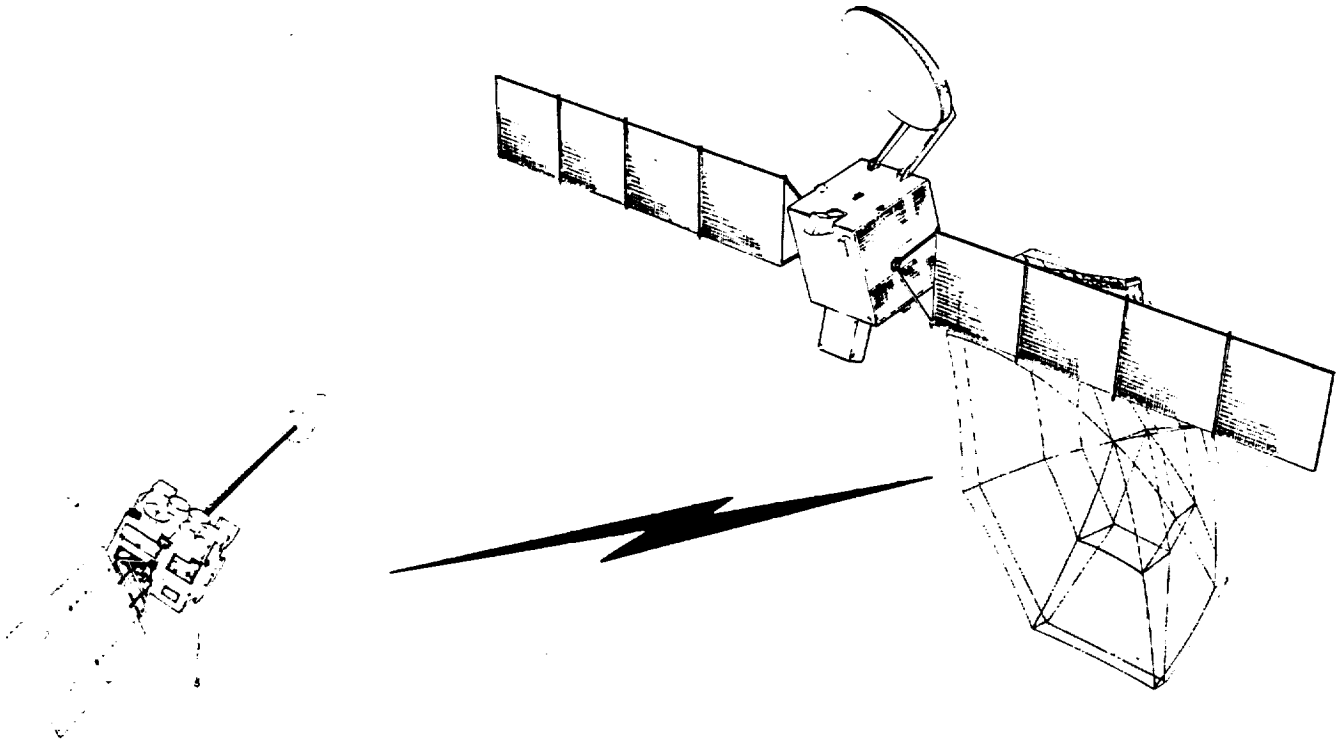

Communications Sciences
Space System Operations
Western Development Laboratories
Ford Aerospace & Communications Corporation
Palo Alto, CA

09-05-86

Addendum A to

NASA 60 GHz Intersatellite Communication Link Definition Study

Modification of Contract NAS5-28589

Mixed Baseband and IF Signals

Communications Sciences
Space Systems Operation
Western Development Laboratories
Ford Aerospace & Communications Corporation
Palo Alto, CA

TABLE OF CONTENTS

ADDENDUM A

MODIFICATION OF CONTRACT

TABLE OF CONTENTS, FIGURES & TABLES

A.1.0 INTRODUCTION

This document is the final report on the 60 GHz channelized Crosslink Study. This study is an extension of the work performed on the 60 GHz Intersatellite Communication Link Definition Study. It addresses a TDAS to TDAS crosslink that accommodates a mixture of frequency translation coherent links and baseband-in/baseband-out links. A 60 GHz communication system will be presented for sizing and analyzing the crosslink. For the coherent links this system translates incoming signals directly up to the 60 GHz band; trunks the signals across from one satellite to a second satellite at 60 GHz then down converts to the proper frequency for re-transmission from the second satellite without converting to any intermediate frequencies. For the baseband-in/baseband-out links the baseband data is modulated on to the 60 GHz carrier at the transmitting satellite and demodulated at the receiving satellite. Throughout this report, the frequency translations coherent links will usually be referred to as "Bent Pipe" links and the baseband-in/ baseband-out links will be referred to as "Mod/Demod" links. Figure A-1 illustrates the relationships of the various users and relay satellites along with the links between them. Table A-1 lists the various services and their characteristics that the TDAS to TDAS crosslink system has been designed to handle.

TABLE A-1
60 GHz Channelized Crosslink Services

RETURN LINKS

LINKS	QTY	TYPE	DATA RATE	MOD.
WSA	5	Mod/Demod	300 Mbps	QPSK
LSA	1	Mod/Demod	1000 Mbps	QPSK
SMA	10	Mod/Demod	0.05 Mbps	QPSK
TT&C	1	Mod/Demod	0.05 Mbps	QPSK
SSA	2	Bent Pipe	12 Mbps	QPSK
KSA	2	Bent Pipe	300 Mbps	QPSK
TT&C	1	Bent Pipe	0.05 Mbps	

FORWARD LINKS

LINKS	QTY	TYPE	DATA RATE	MOD.
WSA	5	Mod/Demod	1 Mbps	QPSK
SMA	2	Mod/Demod	0.01 Mbps	QPSK
LSA	1	Mod/Demod	50 Mbps	QPSK
SSA	2	Bent Pipe	0.3 Mbps	QPSK
KSA	2	Bent Pipe	25 Mbps	QPSK
TT&C	1	Bent Pipe	0.01 Mbps	

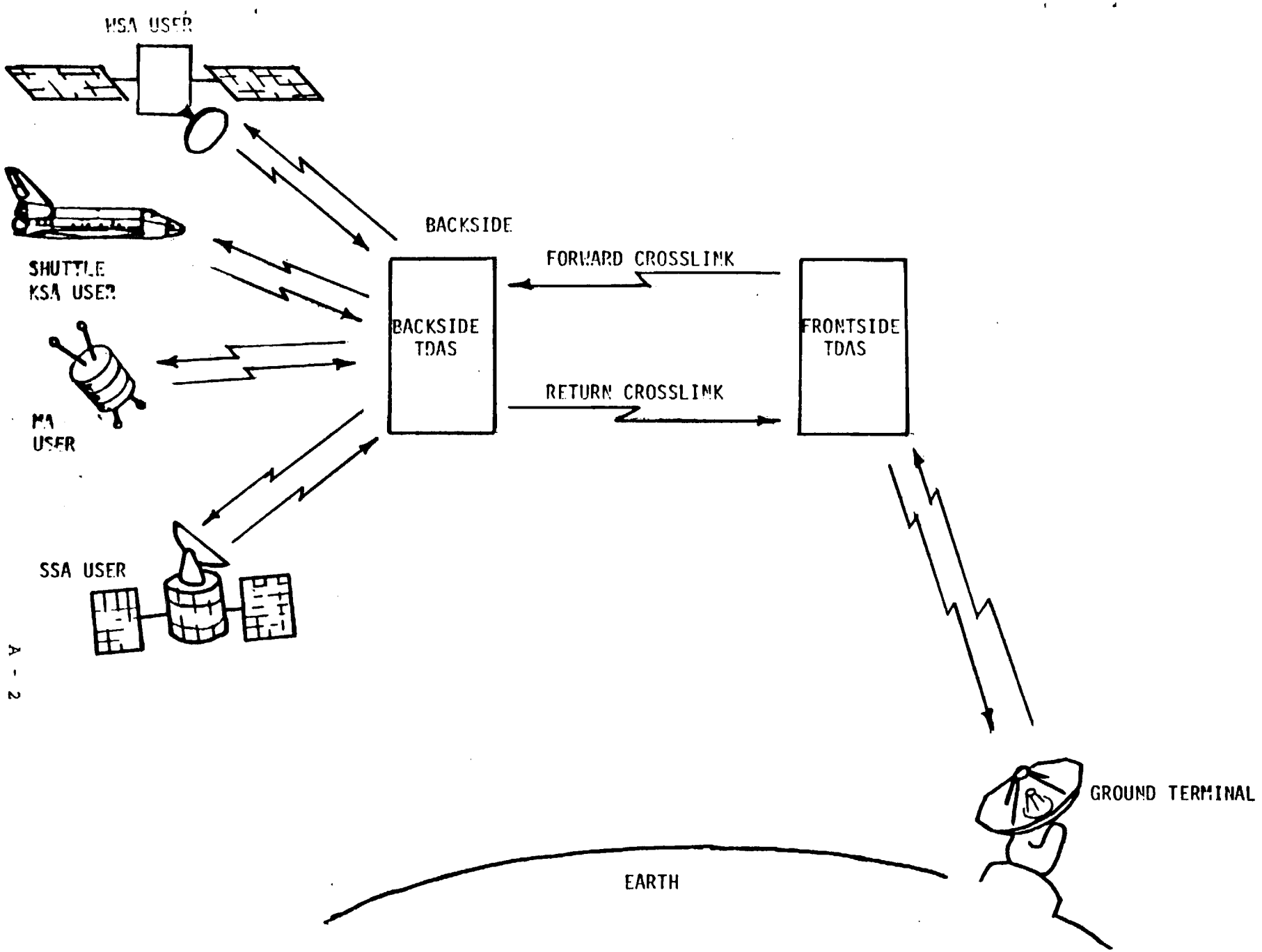

60 GHZ CHANNELIZED CROSSLINK

Figure A-1

A.2.0 FREQUENCY PLAN

For the channelized 60 GHz crosslink system, the WARC frequency band(s) in the 60 GHz range have been broken into fourteen 300 MHz channels with 425 MHz separation between them (the frequency plan is detailed in Figure A-2). The first channel (lowest in frequency) is the Forward channel, the second is the LEO-GEO, and the Return channels follow. There are five allocated channels for WSA, four for LSA, and two for KSA.

The last channel is for the GEO-LEO transmitter. The low data rate on this link requires a bandwidth of only 2 MHz. Therefore, the operating frequency can be offset from the channel center.

Separation of the Forward and Return links by the "LEO-GEO" channel helps to minimize the dangers of intermods in the antenna. Antenna intermods, when they occur, are usually caused by some hardware discontinuity such as poorly-mated flanges and the probability of an occurrence is very low. However, the given separation will preclude any 3rd order products from the Return transmitters falling into the Backside satellite's Forward receiver.

The five WSA channels consist of the W-band LEO-GEO return link data which was received, decoded, and demodulated by the Backside satellite, then modulated on to one of the crosslink channels. Each channel consists of up to 300 Mbps of baseband data.

The LSA return link data is from the laser telescope and the data rate is 1 Gbps. Although the data type (IF modulated or baseband) has not yet been defined, it is assumed for this task that it is baseband. The LSA data has been divided into four groups for transmission over the crosslink. Three groups of 300 Mbps each are sent through separate 300 MHz channels and the remaining 100 Mbps is baseband multiplexed with other low data rate links for transmission through a fourth 300 MHz channel. This last channel, LSA4, has enough bandwidth to include the other low data rate links. These links are two SSA channels of 12 Mbps each, ten SMA channels of 50 Kbps each, and one 10 Kbps TT&C channel. Some of the links on the LSA4 channel are mod/demod and the rest are frequency translated bent pipe links.

The two KSA channels are bent pipe channels containing QPSK data. At a rate of 300 Mbps, the main lobe of the spectrum is contained in the 300 MHz channel.

The separation between the KSA2 and the GEO-LEO transmitter is only 330 MHz. The 300 MHz channel containing the GEO-LEO transmitter is centered at 64130 MHz but the transmitter frequency is at 63998 MHz.

The choice of 300 MHz channels was based on a couple of factors. First of all, 300 MHz works well with the data rates and modulation techniques on most of the links and secondly, 300 MHz of bandwidth at 60 GHz is near the minimum filter bandwidth that can be achieved with reasonable loss, fabrication tolerances, and temperature stability.

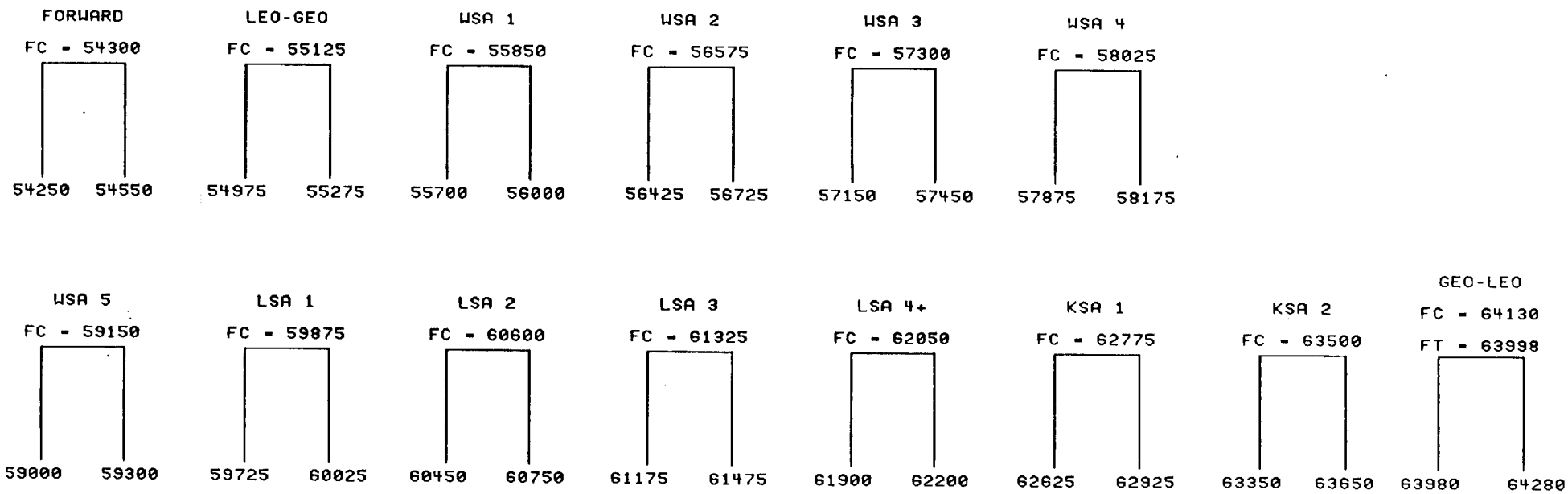

FREQUENCY PLAN

CHANNELIZED 60 GHZ INTERSATELLITE CROSSLINK

Figure A-2

CHANNEL FILTERING

The filtering required to multiplex all fourteen 300 MHz wide channels into the 60 GHz crosslink band must provide sufficient isolation between transmitters and receivers that are co-located in the same spacecraft and must reduce co-channel interference to a negligible level. These two requirements call for increased out of band rejection which drives the filter toward a higher number of poles and narrower passbands. On the other hand, communication performance also needs filters that introduce a minimum of inter-symbol interference (ISI) and have minimum insertion loss. The ISI and insertion loss requirements drive the filter design toward a fewer number of poles and wider passbands. Therefore, a trade-off needed to be performed to define the optimum filters to meet the transmitter rejection, co-channel interference, inter-symbol interference, and insertion loss requirements. To this end, filter design was performed to a sufficient level to determine the feasibility of filters that meet all the requirements.

To accomplish this design and analysis, two existing computer programs were employed. One program analyzes filter distortion and intersymbol interference effects on BPSK/QPSK/SQPSK/MSK signals. The other program models the filters and predicts their RF performance in terms of rejection and passband performance including group delay and insertion loss. Various filters were analyzed in the transmit and receive portions of the link including a 2-pole 150 MHz wide data detection filter. Based on this investigation, 5-pole Chebyschev filters were selected for RF multiplexing the fourteen 300 MHz channels into the 60 GHz band. 3-pole filters gave lower insertion loss and lower ISI, but did not provide adequate isolation between adjacent channels. 7-pole filters provided better isolation between channels but caused more ISI degradation and higher insertion loss. Figure A-3 show the frequency response of the 5-pole filters for the three highest frequency channels. The filters selected have a 300 MHz 0.1 dB ripple bandwidth with a 328 MHz 3-dB bandwidth. With these 5-pole filters, 45 dB of rejection per filter is typically achieved at the point where one filter response crosses over the filter response of the next adjacent channel as shown in Figure A-3. The total isolation between channels at the crossover point is then 90 dB. The only exception is between the two highest frequency channels where the isolation due to filtering at the filter crossover frequency is 76 dB. This is due to the fact that these two channels are only separated by 330 MHz rather than 425 MHz like the rest of the channels. The isolation between the two upper channels is acceptable because one is a TDAS-to-TDAS crosslink channel and the other is a TDAS to LEO channel and the two are not combined on the same antenna. An additional 40 dB of isolation is realized because the channels are not on the same antenna. Assuming an unloaded Q of 4000 the 5-pole EHF filter insertion loss was computed to be 1.6 dB. Although Q's of 4000 are beyond current state-of-the-art, on-going research and development is expected to achieve this by 1989.

The inter-symbol interference degradation of the mod/demod links were analyzed based on a 5-pole transmit filter, a 5-pole receive filter, a 5-pole filter in the down converter and a 2-pole data detection filter. The results of the analysis predict a 1.07 dB degradation on the 300 Mbps links.

Figure A-3

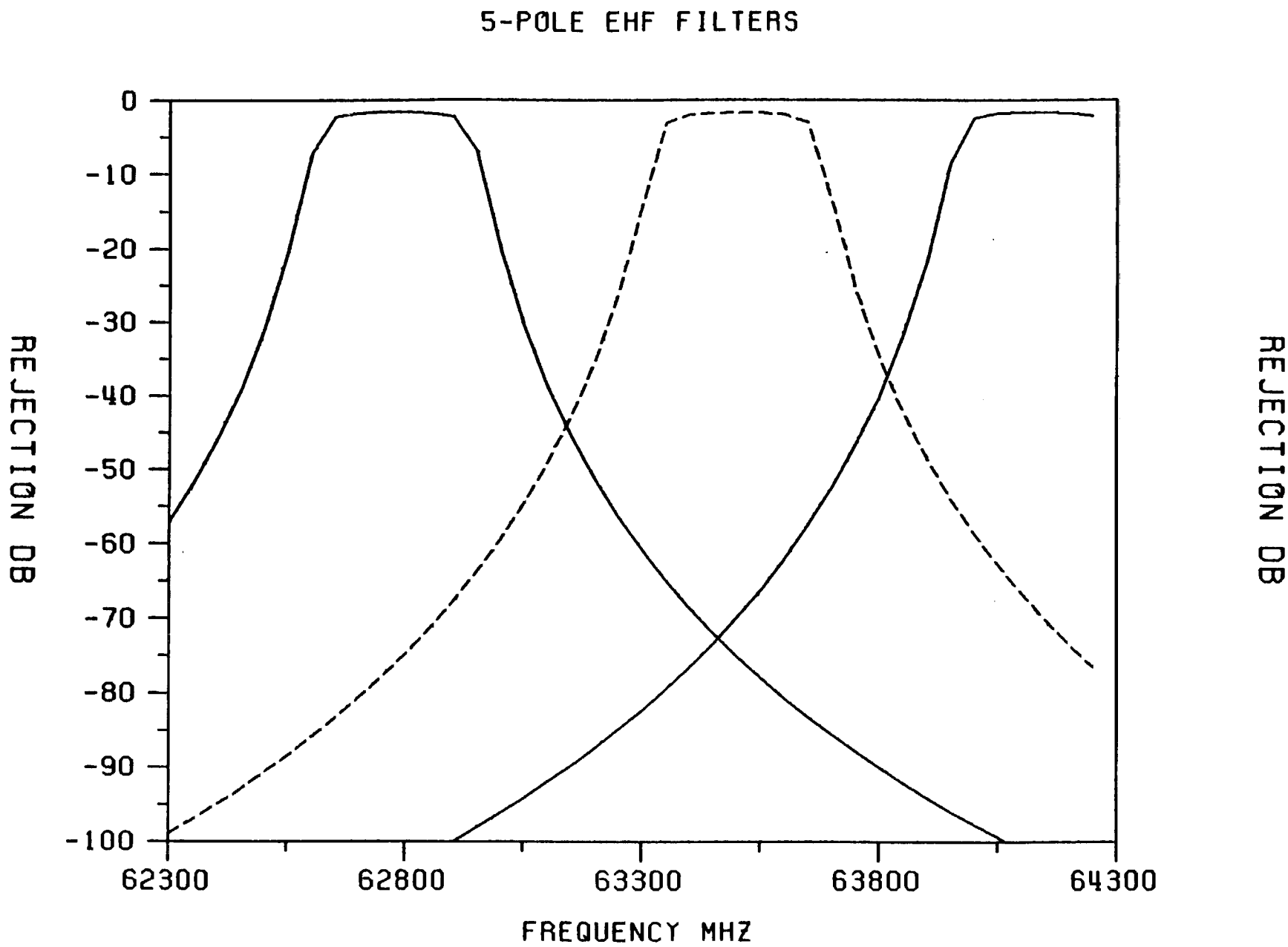

FILTER FREQUENCY RESPONSE FOR THE THREE HIGHEST FREQUENCY CHANNELS

The high amount of attenuation between these channels will result in negligible co-channel interference between any two adjacent channels with similar signal level. The amount of energy from an adjacent channel falling into the filter bandwidth is very small--the S/I is about 64 dB resulting in no co-channel interference.

On the Backside satellite there are two areas of concern. One of these is the possibility of the WSA1 transmitter leaking into the LEO-GEO receiver. If the power of the WSA1 transmitter is 2.5 watts, the 76 dB rejection by the receiver filter added to the 40 dB antenna isolation results in a maximum power at the receiver due to that transmitter of -112 dBW. The power level at the input to the LEO-GEO receiver (see Block diagrams in Attachment #5 of February MPR) is -105.6 dBW. The modulation spectral factor for QPSK is 22 dB. Thus the S/I at the input to the receiver is 28 dB, which results in a degradation due to co-channel interference of about 0.3 dB.

The other area of concern is the co-channel interference between the GEO-LEO transmitter and the KSA2 transmitter. The KSA2 channel is transmitted from a different antenna than the GEO-LEO channel, however, it is possible for the higher altitude LEO satellites to be within the main beam of the GEO-GEO crosslink. In this case, the KSA2 channel has 18.75 dB more EIRP than the GEO-LEO channel. To evaluate the amount of co-channel interference, the power spectral density of the KSA2 channel was adjusted by the attenuation factors of the KSA2 transmit filter and the LEO receive filter, then integrated over the GEO-LEO channel bandwidth. The results of the computation shows the amount of KSA2 power falling into the GEO-LEO channel to be 76.5 dB below the total KSA2 transmit power. Therefore, the S/I ratio of 57.75 dB presents negligible co-channel interference.

A.3.0 CHANNELIZED CROSSLINK COMMUNICATION EQUIPMENT DIAGRAMS

Figures A-4 and A-5 are the Communications Equipment Diagrams for the Frontside TDAS and the Backside TDAS respectively. Each of the services can be traced through a channel from its injection point on one satellite to its output (baseband or RF) at the receiving satellite. The RF multiplexers and demultiplexers are made up of the eleven 5-pole filters combined into a manifold. These filters have been discussed previously in the section on channel filtering.

The tracking and acquisition receivers are shown connected to the TT&C channel; however, they can be connected to any of the channels as long as there is always a carrier present.

Each link has its own power amplifier, low noise amplifier, and up and down converters. This is to avoid intermodulation problems that would result from putting multiple links through a single non-linear item of equipment. For example, the LSA4 channel carries within its 300 MHz passband four sub-channels. Figure A-6 illustrates the usage of this channel. Similarly, Figure A-7 show the utilization of the Forward Channel. If these sub-channels were multiplexed prior to amplification, the amplifier would need to be very linear in order to minimize intermodulation products and cross products which fall many places within the 300 MHz passband. Figure A-8 is the transfer curve of a typical 60 GHz 1 watt IMPATT diode amplifier. Clearly it is not practical to transmit multiple carriers through such a non-linear amplifier. Therefore, a multiplexing method was used that provides separate power amplifiers for each carrier, then combines the amplified signals at 60 GHz. This method avoids using bandpass filters which would have excessive insertion loss for such narrow passbands. The multiplexing of the Forward Channel and the LSA4 Channel is shown in Figures A-9 and A-10 respectively. The RF losses through the multiplexing circuitry is estimated to be between 1.2 dB and 1.5 dB depending on the number of passes through circulators that the various channels must make.

In order to do link calculations, it is necessary to assess feed and network losses. Table A-2 below tabulates the losses of the RF portions of the 60 GHz Crosslink system.

TABLE A-2
FEED AND NETWORK LOSS ASSESSMENT
(IN DB)
CHANNELIZED 60 GHz CROSSLINK

	GEO/GEO	
ITEM	XMIT	RCVR
SWITCH	0.1	0.1
OUTPUT FILTER	1.6	
INPUT FILTER		1.6
COUPLER		0.2
SEPTUM POLARIZER	0.2	0.2
HORN COUPLER	0.1	0.1
WAVEGUIDE (0.25 M)	0.3	0.3
NETWORK TOTAL	2.3	2.5
BEAM WAVEGUIDE	0.6	0.6

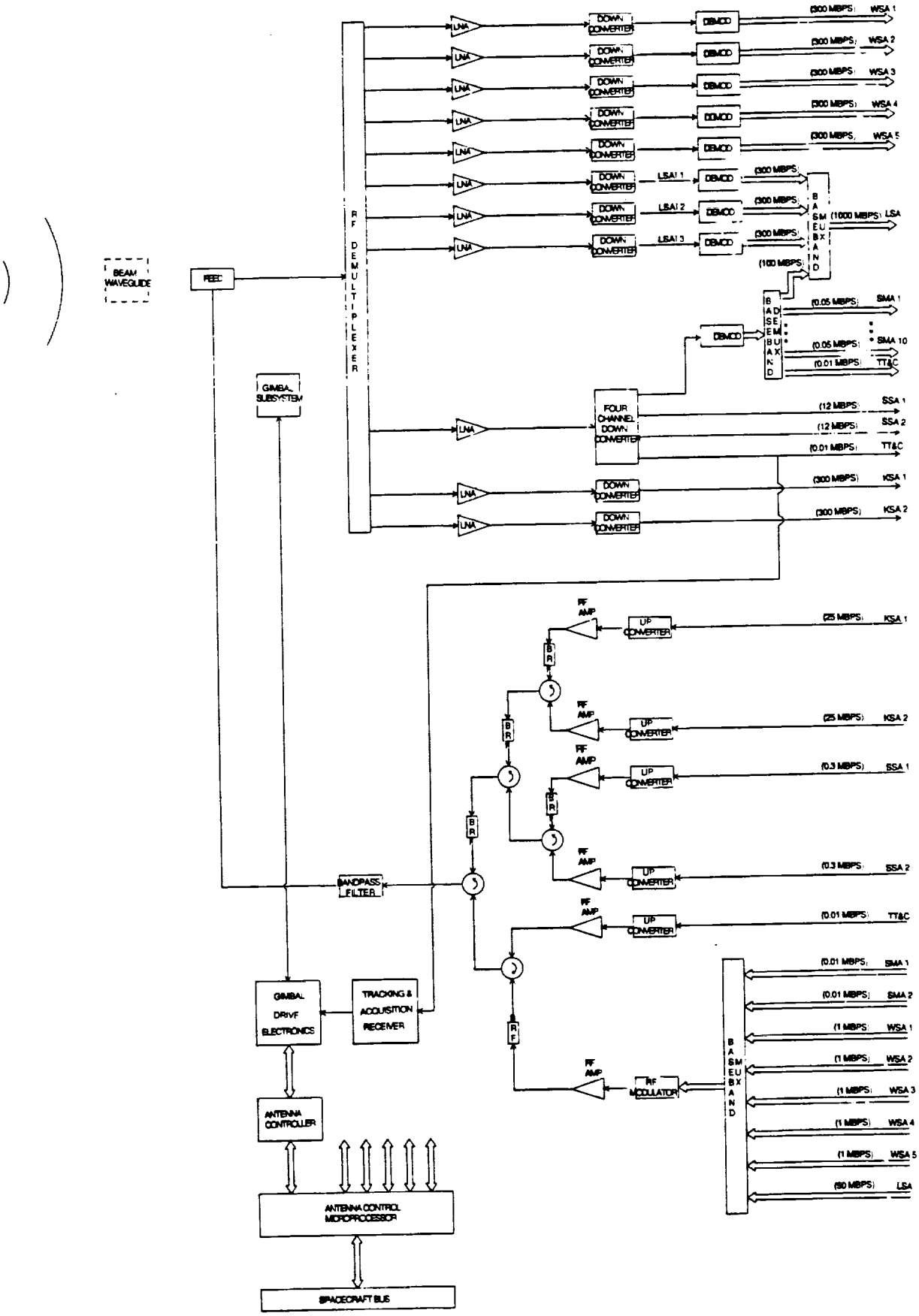

Figure A-4

FRONTSIDE SATELLITE EQUIPMENT

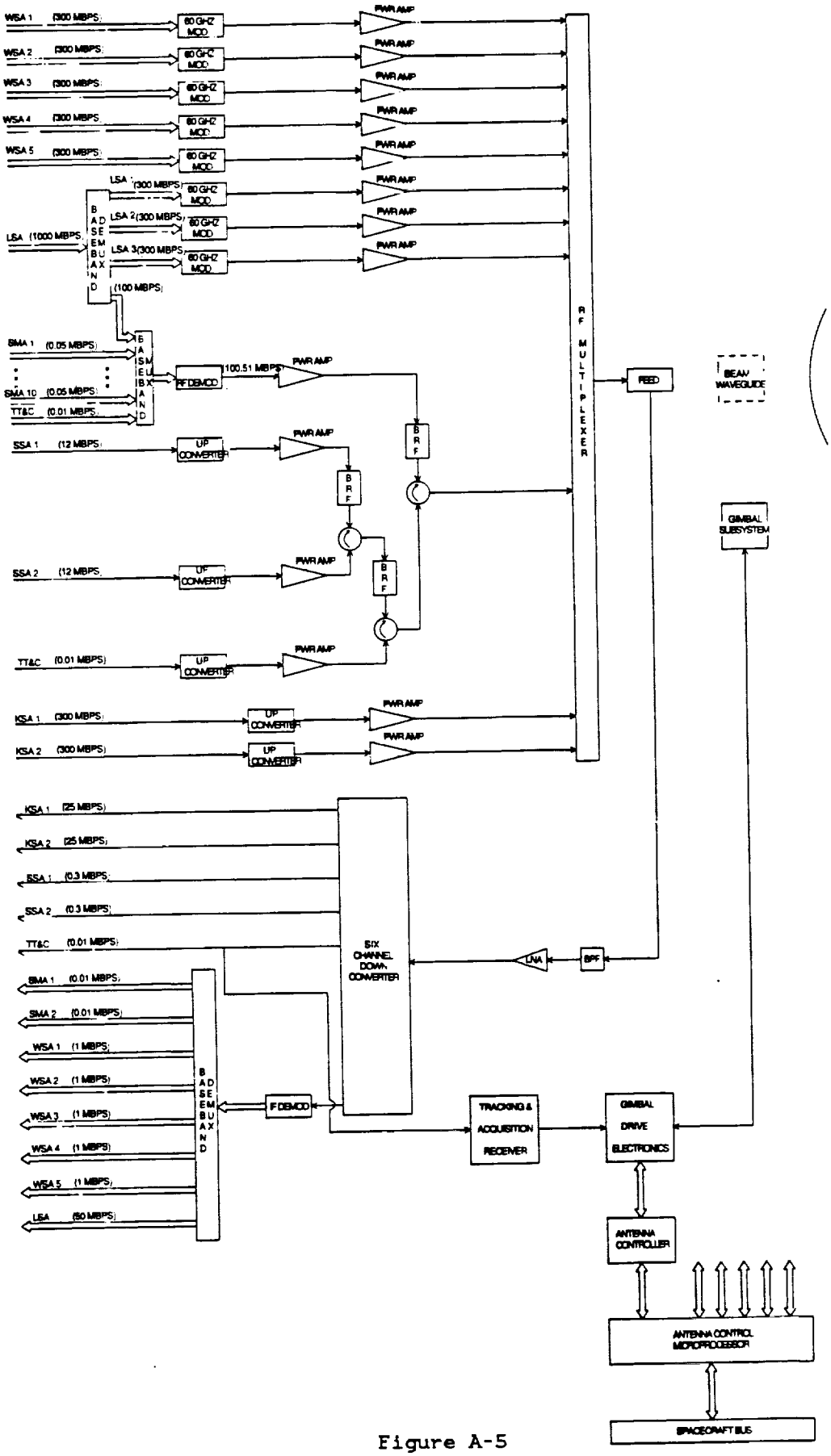

Figure A-5

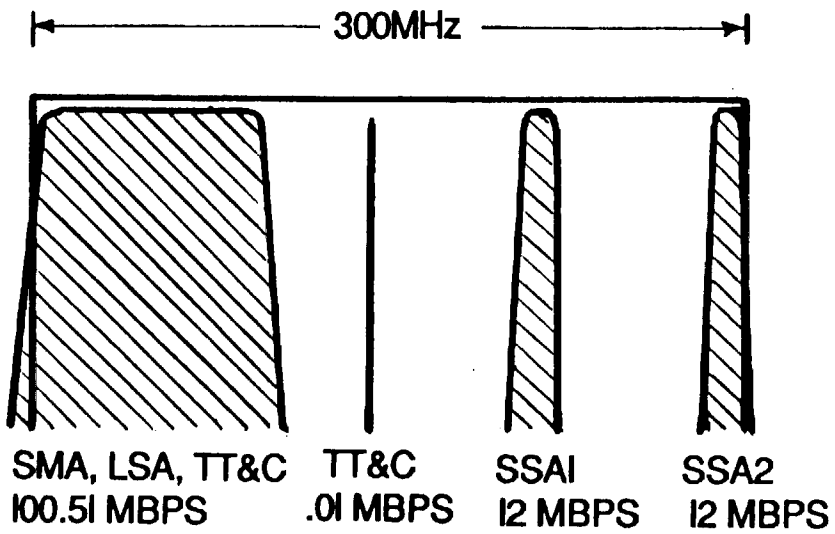

Figure A-6

LSA4 CHANNEL UTILIZATION

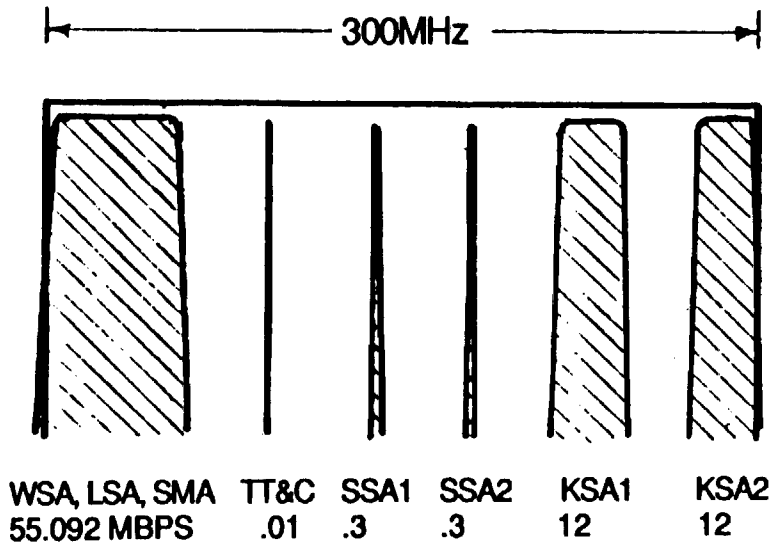

Figure A-7

FORWARD CHANNEL UTILIZATION

POWER TRANSFER CHARACTERISTIC OF COMPLETE TWO-STAGE IMPATT AMPLIFIER

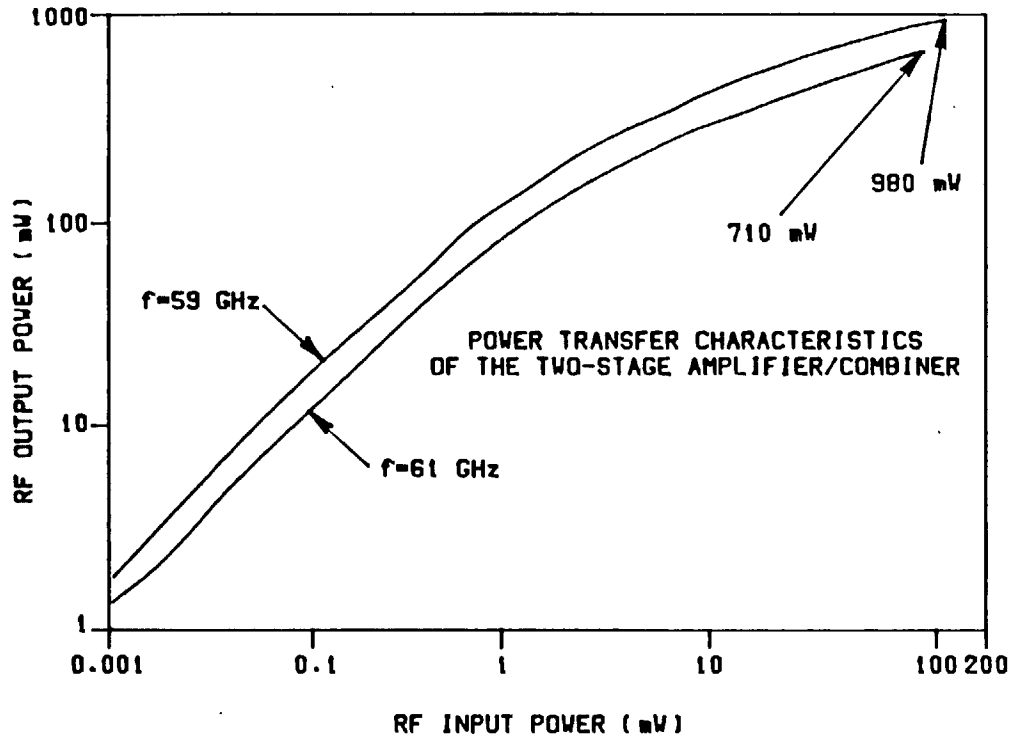

Figure A-8

Reference: H.J. Kuno and D.L. English, "Millimeter Wave IMPATT Power Amplifier/Combiner", IEEE Trans. Microwave Theory Tech., Vol. MTT-24, p.p. 758-767, Nov. 1976.

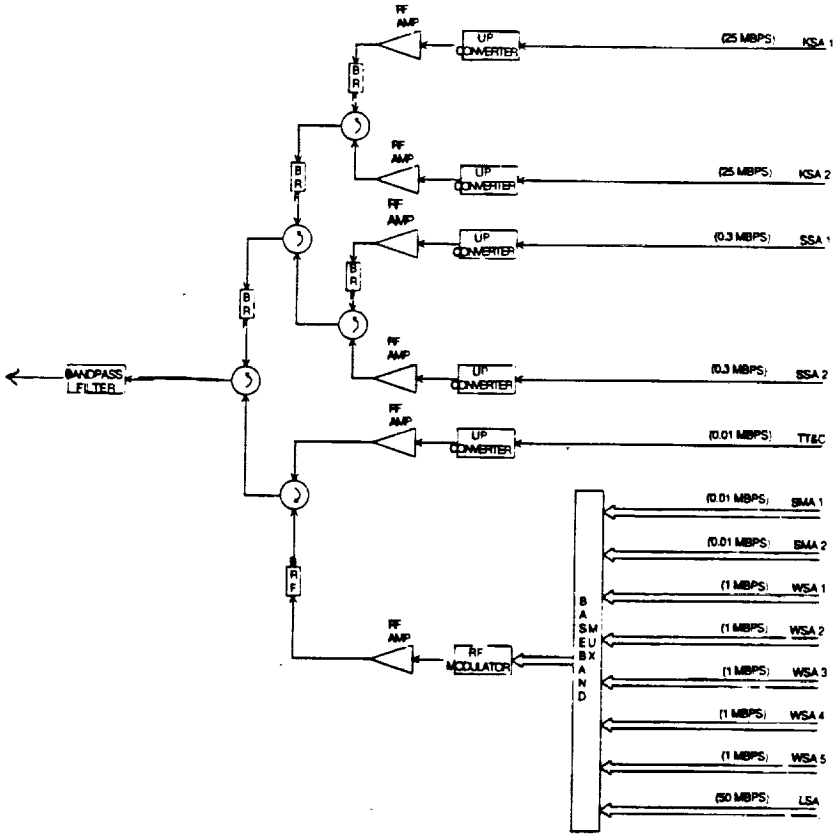

FIGURE A-9

FORWARD CHANNEL TRANSMIT MULTIPLEXING

(FRONTSIDE SATELLITE)

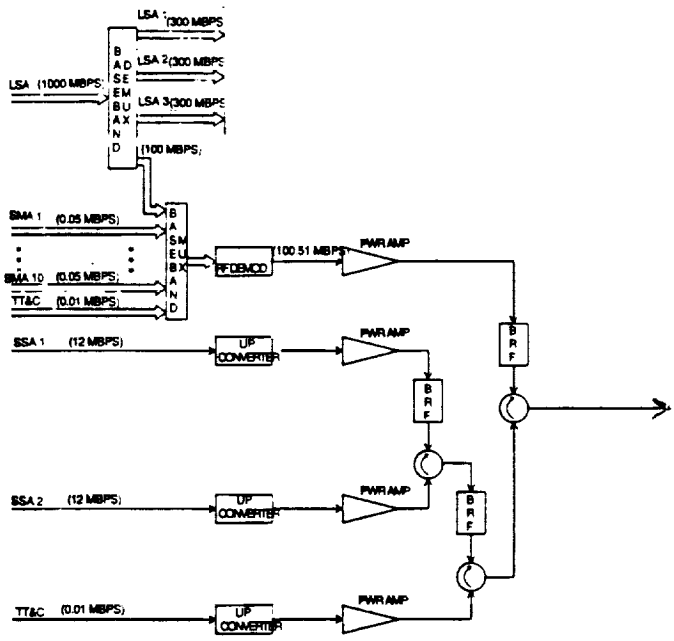

FIGURE A-10

LSA4 CHANNEL TRANSMIT MULTIPLEXING

(BACKSIDE SATELLITE)

A.4.0 LINK CALCULATIONS

This section of this report contains link calculations for each of the services carried on the 60 GHz Channelized Crosslink. The calculations for modulate/ demodulate links are presented somewhat differently from the bent pipe link calculations.

The modulate/demodulate link calculations were performed to support a bit error rate (BER) of less than 10^{-6} between the transmitting and receiving satellites after accounting for all the link degradations. The power amplifiers were sized accordingly.

The calculations for the bent pipe links are more complex because they involve not only the crosslink but also the user-to-TDAS link and the TDAS-to-ground links or vice versa. Figure A-11 illustrates the links involved for a Return bent pipe link. From the equation in Figure A-11 it can be seen that the carrier to noise ratio at the ground terminal is a function of the carrier to noise ratio on the userlink, the power to noise characteristic of the crosslink and the power to noise ratio of the down link. The bent pipe link calculations contain calculations of $(C/N)_{userlink}$, $(P/N)_{crosslink}$, and $(P/N)_{downlink}$.

The $(C/N)_{userlink}$ and $(P/N)_{downlink}$ information for the Return links was obtained from "TDRSS Telecommunications Performance and Interface Document (TPID)" SE-09 12 March 1984. It should be noted that the calculation for the KSA and SSA return links both show negative margins for a BER of 10^{-5}. It is possible to eliminate this negative margin by increasing the outputs of the crosslink power amplifiers. However, to even get back to zero margin requires excessively high power outputs from the 60 GHz amplifiers. The prudent approach to improving the total link performance is to improve the C/N of the user links since they are the poorest links. Improvement in the poorest links produces the maximum improvement in the total link. Therefore, the bent pipe crosslink power amplifiers have been sized large enough not to be the limiting factors in link performance but not so large as to present realizability and reliability problems.

In the case of the Forward bent pipe links, all the necessary parameters to evaluate the uplinks and user forward links were not obtained. The approach to sizing the power amplifiers for these links was to design for a crosslink P/N ratio large enough to support channels with BER better than 10^{-6} given adequate uplink and user forward link performance.

Figures A-12 through A-21 are the detailed calculations for each service supported by the 60 GHz channelized crosslink. Table A-3 summarizes the link characteristics.

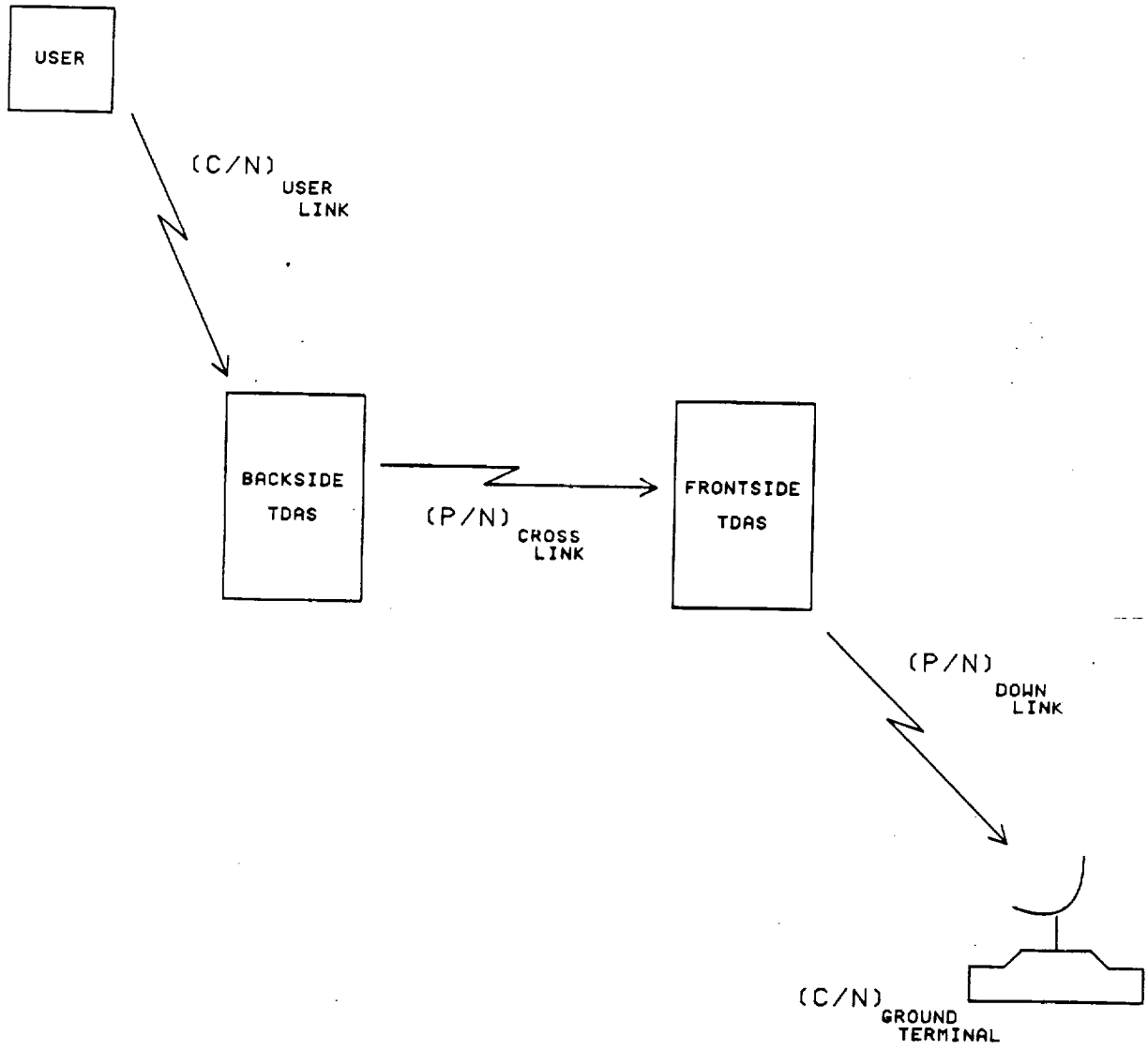

$$\frac{1}{(C/N)_{\substack{\text{GROUND}\\\text{TERMINAL}}}} = \frac{1}{(C/N)_{\substack{\text{USER}\\\text{LINK}}}} + \frac{1}{(P/N)_{\substack{\text{CROSS}\\\text{LINK}}}} + \frac{1}{(P/N)_{\substack{\text{DOWN}\\\text{LINK}}}}$$

BENT PIPE NODAL CONFIGURATION

FIGURE A-11

Figure A-12

WSA1 Channel without Sun Effect

Modulation: QPSK
Coding: None

Carrier Frequency = 55.8 GHz

Parameter	Value	Units	Remarks
Transmitting S/C Power	3.98	dBW	2.5 watts
Transmit Line Loss	2.30	dB	
Feed Loss	0.60	dB	
Transmitting Antenna Gain	63.40	dBi	3.2-m dish
EIRP	64.48	dBW	
Free Space Loss	225.78	dB	83,043 km
Pointing Loss	0.33	dB	0.02 degree
Polarization Loss	0.20	dB	
Tracking Loss	0.33	dB	0.02 degree
Net Path Loss	226.64	dB	
Receiving S/C Antenna Gain	63.40	dBi	3.2-m dish; Temp. = 10 K
Feed Loss	0.60	dB	Temp.= 10 K
Receive Line Loss	2.50	dB	Temp.= 290 K
Receiver Temperature			360 K
System Noise Temperature	26.92	dB-K	492.5 K at Receiver Input
Effective G/T	33.38	dB/K	
Received Carrier Level	-101.86	dBW	At Receiver Input
Boltzmann's Constant	-228.60	dBW/Hz-K	
Received C/No	99.82	dB-Hz	
CCI Degradation	0.00	dB	
ISI Degradation	1.07	dB	
Modem Loss	2.00	dB	
Data Rate	84.77	dB-Hz	300 Mb/s
Available Eb/No	11.98	dB	
Required Eb/No	10.50	dB	BER = 10^{-6}, uncoded
Coding Gain	0.00	dB	
Eb/No Margin	1.48	dB	

Figure A-13

LSA1 Channel without Sun Effect

Modulation: QPSK
Coding: None

Carrier Frequency = 59.9 GHz

Parameter	Value	Units	Remarks
Transmitting S/C Power	3.98	dBW	2.5 watts
Transmit Line Loss	2.30	dB	
Feed Loss	0.60	dB	
Transmitting Antenna Gain	64.00	dBi	3.2-m dish
EIRP	65.08	dBW	
Free Space Loss	226.38	dB	83,043 km
Pointing Loss	0.33	dB	0.02 degree
Polarization Loss	0.20	dB	
Tracking Loss	0.33	dB	0.02 degree
Net Path Loss	227.24	dB	
Receiving S/C Antenna Gain	64.00	dBi	3.2-m dish; Temp. = 10 K
Feed Loss	0.60	dB	Temp.= 10 K
Receive Line Loss	2.50	dB	Temp.= 290 K
Receiver Temperature			360 K
System Noise Temperature	26.92	dB-K	492.5 K at Receiver Input
Effective G/T	33.98	dB/K	
Received Carrier Level	-101.26	dBW	At Receiver Input
Boltzmann's Constant	-228.60	dBW/Hz-K	
Received C/No	100.41	dB-Hz	
CCI Degradation	0.00	dB	
ISI Degradation	1.07	dB	
Modem Loss	2.00	dB	
Data Rate	84.77	dB-Hz	300 Mb/s
Available Eb/No	12.57	dB	
Required Eb/No	10.50	dB	BER = 10^{-6}, uncoded
Coding Gain	0.00	dB	
Eb/No Margin	2.07	dB	

Figure A-14

L8A4 Channel without Sun Effect; Baseband Signals

Modulation: QPSK
Coding: None

Carrier Frequency = 62.0 GHz

Parameter	Value	Units	Remarks
Transmitting S/C Power	0.00	dBW	1.0 watts
Transmit Line Loss	3.80	dB	
Feed Loss	0.60	dB	
Transmitting Antenna Gain	64.20	dBi	3.2-m dish
EIRP	59.80	dBW	
Free Space Loss	226.69	dB.	83,043 km
Pointing Loss	0.33	dB	0.02 degree
Polarization Loss	0.20	dB	
Tracking Loss	0.33	dB	0.02 degree
Net Path Loss	227.55	dB	
Receiving S/C Antenna Gain	64.20	dBi	3.2-m dish; Temp. = 10 K
Feed Loss	0.60	dB	Temp.= 10 K
Receive Line Loss	2.50	dB	Temp.= 290 K
Receiver Temperature			360 K
System Noise Temperature	26.92	dB-K	492.5 K at Receiver Input
Effective G/T	34.18	dB/K	
Received Carrier Level	-106.65	dBW	At Receiver Input
Boltzmann's Constant	-228.60	dBW/Hz-K	
Received C/No	95.02	dB-Hz	
CCI Degradation	0.00	dB	
ISI Degradation	1.07	dB	
Modem Loss	2.00	dB	
Data Rate	80.04	dB-Hz	101 Mb/s
Available Eb/No	11.91	dB	
Required Eb/No	10.50	dB	BER = 10^{-6}, uncoded
Coding Gain	0.00	dB	
Eb/No Margin	1.41	dB	

SSA RETURN
USER TO BACKSIDE TO FRONTSIDE TO GROUND
12 MBPS; NO CODING; CARRIER FREQUENCY: 62.050 GHz

1.	USER EIRP, DBW	40.99	(Note 1)
2.	SPACE LOSS, DB	192.20	(Note 1)
3.	TDRSS G/T, DB/K	8.57	(Note 1)
4.	SIGNAL SUPPRESSION, DB	0.00	(Note 1)
5.	BOLTZMANNS CONST, DBW/HZ-K	-228.60	(Note 1)
6.	C/No AT BACKSIDE, DB-HZ	85.96	(Note 1)
7.	BANDWIDTH, DB-HZ	71.94	(Note 1)
8.	C/N AT BACKSIDE, DB-HZ	14.02	(Note 1)
9.	BACKSIDE-CROSSLINK EIRP, DBW	59.56	(Note 2)
10.	PATH LOSS, DB	-226.69	(83,043 KM)
11.	POLARIZATION LOSS, DB	.20	
12.	POINTING LOSS, DB	.33	
13.	TRACKING LOSS, DB	.33	
14.	FRONTSIDE-CROSSLINK REC. POWER DBI	-167.99	
15.	FRONTSIDE-CROSSLINK G/T, DB/K	34.24	(Note 3)
16.	BOLTZMANNS CONST, DBW/HZ-K	-228.60	
17.	P/No (THERMAL), DB-HZ	94.85	
18.	P/No (TOTAL) DB-HZ	94.85	
19.	BANDWIDTH, DB-HZ	71.94	
20.	P/N (TOTAL), DB	22.91	
21.	FRONTSIDE-DOWNLINK EIRP DBW	39.90	(Note 1)
22.	PATH LOSS, DB	207.70	(Note 1)
23.	ATMOSPHERIC LOSS, DB	1.10	(Note 1)
24.	POLARIZATION LOSS	.03	(Note 1)
25.	RAIN ATTENUATION, DB	6.00	(Note 1)
26.	GROUND RECEIVED POWER, DBI	-174.93	(Note 1)
27.	GROUND G/T, DB/K	41.70	(Note 1)
28.	BOLTZMANNS CONST, DBW/HZ-K	-228.60	(Note 1)
29.	P/No (THERMAL), DB-HZ	75.37	(Note 1)
30.	IM DEGRADATION, DB	1.22	(Note 1)
31.	P/No (TOTAL), DB-HZ	94.15	(Note 1)
32.	BANDWIDTH, DB-HZ	71.94	(Note 1)
33.	P/N (TOTAL), DB	22.21	(Note 1)
34.	C/N AT GROUND, DB	12.95	
35.	BANDWIDTH, DB-HZ	71.94	(Note 1)
36.	C/No AT GROUND, DB-HZ	84.89	
37.	DATA RATE, DB-BPS (300 MBPS)	70.79	(Note 1)
38.	Eb/No INTO DEMODULATOR, DB	14.10	
39.	GROUND EQUIPMENT DEG., DB	4.50	(Note 1)
40.	DIFF CODING LOSS, DB	.30	(Note 1)
41.	NET Eb/No, DB	9.30	
42.	THEORETICALLY REQUIRED Eb/No, DB	9.60	(Note 1)
43.	MARGIN WITH RAIN	-0.30	

NOTES:

1) Values obtained from "TDRSS Telecommunications Performance and Interface Document (TPID)"

SE-09 12 March 1984 Table 1.1.1-3 page 1-9.

2) SSA Return Crosslink EIRP:

Transmitter Power, dBW	0.00
Combiner Loss, dB	-1.80
Transmission Line Loss, dB	-2.30
Feed Loss, dB	- .60
Transmit Antenna Gain, dBi	66.36
Antenna Efficiency, dB	-2.10
EIRP	59.56 dBW

3) SSA Return Crosslink G/T:

Receive Antenna Gain, dBi	66.36
Antenna Efficiency, dB	-2.10
Feed Loss, dB	-.60
Receive Line Loss, dB	-2.50
System Noise Temperature, dB-K	-26.92
G/T	34.24 dB/K

Figure A-15

KSA RETURN
USER TO BACKSIDE TO FRONTSIDE TO GROUND
300 MBPS; NO CODING; CARRIER FREQUENCY: 62.775 GHz

1.	USER EIRP, DBW	57.37	(Note 1)
2.	SPACE LOSS, DB	209.20	(Note 1)
3.	TDRSS G/T, DB/K	23.94	(Note 1)
4.	BOLTZMANNS CONST, DBW/HZ-K	-228.60	(Note 1)
5.	C/No AT BACKSIDE, DB-HZ	100.71	(Note 1)
6.	BANDWIDTH, DB-HZ	83.73	(Note 1)
7.	C/N AT BACKSIDE, DB-HZ	16.98	(Note 1)
8.	BACKSIDE-CROSSLINK EIRP, DBW	67.46	(Note 2)
9.	PATH LOSS, DB	-226.78	(83,043 KM)
10.	POLARIZATION LOSS, DB	.20	
11.	POINTING LOSS, DB	.33	
12.	TRACKING LOSS, DB	.33	
13.	FRONTSIDE-CROSSLINK REC. POWER DBW	-160.18	
14.	FRONTSIDE-CROSSLINK G/T, DB/K	34.34	(Note 3)
15.	BOLTZMANNS CONST, DBW/HZ-K	-228.60	
16.	P/No (THERMAL), DB-HZ	102.76	
17.	P/No (TOTAL) DB-HZ	102.76	
18.	BANDWIDTH, DB-HZ	83.73	
19.	P/N (TOTAL), DB	19.03	
20.	FRONTSIDE-DOWNLINK EIRP DBW	52.90	(Note 1)
21.	PATH LOSS, DB	207.70	(Note 1)
22.	ATMOSPHERIC LOSS, DB	1.10	(Note 1)
23.	POLARIZATION LOSS	.03	(Note 1)
24.	RAIN ATTENUATION, DB	6.00	(Note 1)
25.	GROUND RECEIVED POWER, DBI	-161.93	(Note 1)
26.	GROUND G/T, DB/K	41.00	(Note 1)
27.	BOLTZMANNS CONST, DBW/HZ-K	-228.60	(Note 1)
28.	P/No (THERMAL), DB-HZ	107.67	(Note 1)
29.	CROSS POL. DEG., DB	.47	(Note 1)
30.	P/No (TOTAL), DB-HZ	107.20	(Note 1)
31.	BANDWIDTH, DB-HZ	83.73	(Note 1)
32.	P/N (TOTAL), DB	23.47	(Note 1)
33.	C/N AT GROUND, DB	14.31	
34.	BANDWIDTH, DB-HZ	83.73	(Note 1)
35.	C/No AT GROUND, DB-HZ	98.04	
36.	DATA RATE, DB-BPS (300 MBPS)	84.77	(Note 1)
37.	Eb/No INTO DEMODULATOR, DB	13.27	
38.	GROUND EQUIPMENT DEG., DB	4.05	(Note 1)
39.	DIFF CODING LOSS, DB	.30	(Note 1)
40.	NET Eb/No, DB	8.92	
41.	THEORETICALLY REQUIRED Eb/No, DB	9.60	(Note 1)
42.	MARGIN WITH RAIN	-0.68	

NOTES:

1) Values obtained from "TDRSS Telecommunications Performance and Interface Document (TPID)"

SE-09 12 March 1984 Table 1.1.1-4 page 1-11.

2) KSA Return Crosslink EIRP:

Transmitter Power, dBW	6.00
Transmission Line Loss, dB	-2.30
Feed Loss, dB	- .60
Transmit Antenna Gain, dBi	66.46
Antenna Efficiency, dB	-2.10
EIRP	67.46 dBW

3) KSA Return Crosslink G/T:

Receive Antenna Gain, dBi	66.46
Antenna Efficiency, dB	-2.10
Feed Loss, dB	-.60
Receive Line Loss, dB	-2.50
System Noise Temperature, dB-K	-26.92
G/T	34.34 dB/K

Figure A-16

TT&C RETURN
BACKSIDE TO FRONTSIDE TO GROUND
10 Kbps: NO CODING: CARRIER FREQUENCY: 62.050 GHz

1.	BACKSIDE-CROSSLINK EIRP, DBW	49.86	(Note 2)	
2.	PATH LOSS, DB	-226.69	(83.043 KM)	
3.	POLARIZATION LOSS, DB	.20		
4.	POINTING LOSS, DB	.33		
5.	TRACKING LOSS, DB	.33		
6.	FRONTSIDE-CROSSLINK REC. POWER DBI	-166.83		
7.	FRONTSIDE-CROSSLINK G/T, DB/K	34.24	(Note 3)	
8.	BOLTZMANNS CONST, DBW/HZ-K	-228.60		
9.	C/No (THERMAL), DB-HZ	96.01		
10.	C/No (TOTAL) DB-HZ	96.01		
11.	BANDWIDTH, DB-HZ	64.77	(Note 1)	
12.	C/N (TOTAL), DB	21.24		
13.	FRONTSIDE-DOWNLINK EIRP DBW	28.52	(Note 1)	
14.	PATH LOSS, DB	207.43	(Note 1)	
15.	ATMOSPHERIC LOSS, DB	1.30	(Note 1)	
16.	POLARIZATION LOSS	0.00	(Note 1)	
17.	RAIN ATTENUATION, DB	15.00	(Note 1)	
18.	GROUND RECEIVED POWER, DBI	-195.21	(Note 1)	
19.	GROUND G/T, DB/K	41.40	(Note 1)	
20.	BOLTZMANNS CONST, DBW/HZ-K	-228.60	(Note 1)	
21.	DEG. DUE TO TRANSMIT S/N	.98	(Note 1)	(BW=64.77 dB-HZ) (S/N = 16 dB)
22.	P/No (THERMAL), DB-HZ	73.81	(Note 1)	
23.	TELEMETRY MOD. LOSS, DB	4.58	(Note 1)	
24.	BANDWIDTH, DB-HZ	64.77	(Note 1)	
25.	P/N (TOTAL), DB	4.46	(Note 1)	
26.	C/N AT GROUND, DB	4.37		
27.	BANDWIDTH, DB-HZ	64.77	(Note 1)	
28.	C/No AT GROUND, DB-HZ	69.14		
29.	DATA RATE, DB-BPS (10 KBPS)	40.00	(Note 1)	
30.	RECEIVER LOSS, DB	2.20	(Note 1)	
31.	DEMODULATOR LOSS, DB	1.80	(Note 1)	
32.	RECEIVED SNR, DB	35.14		
33.	REQUIRED SNR, DB	11.00	(Note 1)	
34.	TELEMETRY MARGIN	14.14		

NOTES:

1) Values obtained from "TDRSS Telecommunications Performance and Interface Document (TPID)"

SE-09 12 March 1984 Table 1.3.1-4 page 1-68.

2) TT&C Return Crosslink EIRP:

Transmitter Power, dBW	-10.00
Combiner Loss, dB	-1.50
Transmission Line Loss, dB	-2.30
Feed Loss, dB	- .60
Transmit Antenna Gain, dBi	66.36
Antenna Efficiency, dB	-2.10
EIRP	49.86 dBW

3) TT&C Return Crosslink G/T:

Receive Antenna Gain, dBi	66.36
Antenna Efficiency, dB	-2.10
Feed Loss, dB	-.60
Receive Line Loss, dB	-2.50
System Noise Temperature, dB-K	-26.92
G/T	34.24 dB/K

Figure A-17

Figure A-18

Forward Channel without Sun Effect; Baseband Signals

Modulation: QPSK
Coding: None

Carrier Frequency = 54.3 GHz

Parameter	Value	Units	Remarks
Transmitting S/C Power	0.00	dBW	1.0 watts
Transmit Line Loss	3.80	dB	
Feed Loss	0.60	dB	
Transmitting Antenna Gain	63.10	dBi	3.2-m dish
EIRP	58.70	dBW	
Free Space Loss	225.53	dB	83,043 km
Pointing Loss	0.33	dB	0.02 degree
Polarization Loss	0.20	dB	
Tracking Loss	0.33	dB	0.02 degree
Net Path Loss	226.39	dB	
Receiving S/C Antenna Gain	63.10	dBi	3.2-m dish; Temp. = 10 K
Feed Loss	0.60	dB	Temp.= 10 K
Receive Line Loss	2.50	dB	Temp.= 290 K
Receiver Temperature			360 K
System Noise Temperature	26.92	dB-K	492.5 K at Receiver Input
Effective G/T	33.08	dB/K	
Received Carrier Level	-107.69	dBW	At Receiver Input
Boltzmann's Constant	-228.60	dBW/Hz-K	
Received C/No	93.98	dB-Hz	
CCI Degradation	0.00	dB	
ISI Degradation	1.07	dB	
Modem Loss	2.00	dB	
Data Rate	77.48	dB-Hz	56 Mb/s
Available Eb/No	13.43	dB	
Required Eb/No	10.50	dB	BER = 10^{-6}, uncoded
Coding Gain	0.00	dB	
Eb/No Margin	2.93	dB	

SSA FORWARD
FRONTSIDE TO BACKSIDE
0.3 MBPS; NO CODING; CARRIER FREQUENCY = 54.300 GHz

1.	FRONTSIDE CROSSLINK EIRP, DBW	42.71	(Note 1)
2.	PATH LOSS, DB	-225.52	(83,043 KM)
3.	POLARIZATION LOSS, DB	.20	
4.	POINTING LOSS, DB	.33	
5.	TRACKING LOSS, DB	.33	
6.	BACKSIDE CROSSLINK REC., POWER DBI	-183.67	
7.	BACKSIDE CROSSLINK G/T, DB/K	33.09	(Note 2)
8.	BOLTZMANNS CONST., DBW/HZ-K	-228.60	
9.	P/No (THERMAL), DB-HZ	78.02	
10.	P/No (TOTAL), DB-HZ	78.02	
11.	BANDWIDTH, DB-HZ	55.16	(328 KHz)
12.	P/N (TOTAL), DB	22.86	

NOTES:

1) SSA Forward Crosslink EIRP:

Transmitter Power, dBW	-16.00	(25 mW)
Combiner Loss, dB	-1.50	
Transmission Line Loss, dB	-2.30	
Feed Loss, dB	- .60	
Transmit Antenna Gain, dBi	65.21	
Antenna Efficiency, dB	-2.10	
EIRP	42.71 dBW	

2) SSA Forward Crosslink G/T:

Receive Antenna Gain, dBi	65.21
Antenna Efficiency, dB	-2.10
Feed Loss, dB	-.60
Receive Line Loss, dB	-2.50
System Noise Temperature, dB-K	-26.92
G/T	33.09 dB/K

Figure A-19

KSA FORWARD
FRONTSIDE TO BACKSIDE
25 MBPS; NO CODING; CARRIER FREQUENCY = 54.300 GHz

1.	FRONTSIDE CROSSLINK EIRP, DBW	62.01	(Note 1)
2.	PATH LOSS, DB	-225.52	(83,043 KM)
3.	POLARIZATION LOSS, DB	.20	
4.	POINTING LOSS, DB	.33	
5.	TRACKING LOSS, DB	.33	
6.	BACKSIDE CROSSLINK REC., POWER DBI	-164.37	
7.	BACKSIDE CROSSLINK G/T, DB/K	33.09	(Note 2)
8.	BOLTZMANNS CONST., DBW/HZ-K	-228.60	
9.	P/No (THERMAL), DB-HZ	97.32	
10.	P/No (TOTAL), DB-HZ	97.32	
11.	BANDWIDTH, DB-HZ	73.98	(27.3 MHz)
12.	P/N (TOTAL), DB	23.34	

NOTES:

1) KSA Forward Crosslink EIRP:

Transmitter Power, dBW	3.00 (2 W)
Combiner Loss, dB	-1.20
Transmission Line Loss, dB	-2.30
Feed Loss, dB	- .60
Transmit Antenna Gain, dBi	65.21
Antenna Efficiency, dB	-2.10
EIRP	62.01 dBW

2) KSA Forward Crosslink G/T:

Receive Antenna Gain, dBi	65.21
Antenna Efficiency, dB	-2.10
Feed Loss, dB	-.60
Receive Line Loss, dB	-2.50
System Noise Temperature, dB-K	-26.92
G/T	33.09 dB/K

Figure A-20

TT&C FORWARD
FRONTSIDE TO BACKSIDE
0.01 MBPS; NO CODING; CARRIER FREQUENCY = 54.300 GHz

1.	FRONTSIDE CROSSLINK EIRP, DBW	49.01	(Note 1)
2.	PATH LOSS, DB	-225.52	(83,043 KM)
3.	POLARIZATION LOSS, DB	.20	
4.	POINTING LOSS, DB	.33	
5.	TRACKING LOSS, DB	.33	
6.	BACKSIDE CROSSLINK REC., POWER DBI	-177.37	
7.	BACKSIDE CROSSLINK G/T, DB/K	33.09	(Note 2)
8.	BOLTZMANNS CONST., DBW/HZ-K	-228.60	
9.	P/No (THERMAL), DB-HZ	84.32	
10.	P/No (TOTAL), DB-HZ	84.32	
11.	BANDWIDTH, DB-HZ	40.41	(11 KHz)
12.	P/N (TOTAL), DB	43.91	

NOTES:

1) TT&C Forward Crosslink EIRP:

Transmitter Power, dBW	-10.00 (100 mW)
Combiner Loss, dB	-1.20
Transmission Line Loss, dB	-2.30
Feed Loss, dB	- .60
Transmit Antenna Gain, dBi	65.21
Antenna Efficiency, dB	-2.10
EIRP	49.01 dBW

2) TT&C Forward Crosslink G/T:

Receive Antenna Gain, dBi	65.21
Antenna Efficiency, dB	-2.10
Feed Loss, dB	-.60
Receive Line Loss, dB	-2.50
System Noise Temperature, dB-K	-26.92
G/T	33.09 dB/K

Figure A-21

CHANNELIZED 60 GHz CROSSLINK CHARACTERISTICS SUMMARY
RETURN LINKS

LINK	TYPE	DATE RATE	MOD	POWER AMP	BER	MARGIN
WSA 1	MOD/DEMOD	300 MBPS	QPSK	2.5 W	10^{-6}	1.48 dB*
WSA 2	MOD/DEMOD	300 MBPS	QPSK	2.5 W	10^{-6}	1.70 dB*
WSA 3	MOD/DEMOD	300 MBPS	QPSK	2.5 W	10^{-6}	1.93 dB*
WSA 4	MOD/DEMOD	300 MBPS	QPSK	2.5 W	10^{-6}	2.14 dB*
WSA 5	MOD/DEMOD	300 MBPS	QPSK	2.5 W	10^{-6}	2.48 dB*
LSA 1	MOD/DEMOD	300 MBPS	QPSK	2.5 W	10^{-6}	2.07 dB*
LSA 2	MOD/DEMOD	300 MBPS	QPSK	2.5 W	10^{-6}	2.28 dB*
LSA 3	MOD/DEMOD	300 MBPS	QPSK	2.5 W	10^{-6}	2.49 dB*
LSA 4	MOD/DEMOD	100 MBPS	QPSK			
SMA 1	MOD/DEMOD	0.05 MBPS	QPSK			
o	o	o		1.0 W	10^{-6}	1.41 dB*
SMA 10	MOD/DEMOD	0.05 MBPS	QPSK			
TT&C	MOD/DEMOD	0.01 MBPS	QPSK			
SSA 1	BENT PIPE	12 MBPS	QPSK	1.0 W	10^{-5}	-0.30 dB**
SSA 2	BENT PIPE	12 MBPS	QPSK	1.0 W	10^{-5}	-0.30 dB**
KSA 1	BENT PIPE	300 MBPS	QPSK	4.0 W	10^{-5}	-0.68 dB**
KSA 2	BENT PIPE	300 MBPS	QPSK	4.0 W	10^{-6}	-0.68 dB**
TT&C	BENT PIPE	0.01 MBPS		0.1 W	10^{-5}	14.14 dB **

1000 MBPS

*Backside to frontside crosslink performance only. Does not include given user link or downlink degradation
**Calculated at ground terminal based on User Link/Down Link parameters given in "TDRSS Telecommunications Performance and Interface Document" SE-09 12 March 1984.

FORWARD LINKS

LINK	TYPE	DATA RATE	MOD.	POWER AMP	BER	MARGIN
WSA 1	MOD/DEMOD	1 MBPS	QPSK			
WSA 2	MOD/DEMOD	1 MBPS	QPSK			
WSA 3	MOD/DEMOD	1 MBPS	QPSK			
WSA 4	MOD/DEMOD	1 MBPS	QPSK			
WSA 5	MOD/DEMOD	1 MBPS	QPSK	1.0 W	10^{-6}	2.93 dB*
SMA 1	MOD/DEMOD	0.01 MBPS	QPSK			
SMA 2	MOD/DEMOD	0.01 MBPS	QPSK			
LSA	MOD/DEMOD	50 MBPS	QPSK		P/N	
SSA 1	BENT PIPE	0.3 MBPS	QPSK	0.025 W	22.86 dB*	
SSA 2	BENT PIPE	0.3 MBPS	QPSK	0.025 W	22.86 dB*	
KSA 1	BENT PIPE	25 MBPS	QPSK	2.0 W	23.34 dB*	
KSA 2	BENT PIPE	25 MBPS	QPSK	2.0 W	23.34 dB*	
TT&C	BENT PIPE	0.01 MBPS		0.1 W	43.91 dB*	

*Frontside to Backside crosslink performance only. Does not include user link or up link degradations.

Table A-3

A.5.0 ANALYSIS

AM-to-PM Conversion

AM-to-PM conversion has been considered in the design of crosslink systems. In this study the problem has been addressed; however, a comprehensive analysis was more than could be accomplished within the scope of this study. AM-to-PM Conversion primarily results from having non-constant envelope signals passing through non-linear amplifiers. The solutions to minimizing AM-to-PM are to eliminate the amplitude modulation on the signals and/or to linearize the amplifiers. The primary source of amplitude modulation on the QPSK waveforms is noise. Noise, hence, AM-to-PM should be negligible on the modulate/demodulate links because the inputs to the power amplifiers have a very high signal to noise ratio coming directly from the 60 GHz modulators. On the other hand, the bent pipe links are much more susceptible to AM-to-PM because the inputs to the power amplifiers on those links are the frequency translated signals-plus-noise from other links. This is another reason for improving the signal-to-noise ratios of the user-to-TDAS links. Figure A-22 illustrates the importance of having a good signal-to-noise ratio as an input to the crosslink. This curve (Ref. 1) is based on a soft limiter cascaded with a TWT; however, for illustrative purposes, it is applicable to soft limiting solid state amplifiers as well. To apply this curve to the Return links of 60 GHz channelized crosslink the "Uplink SNR" on Figure A-22 corresponds to the user link SNR or (C/N). The ordinate marked "Downlink SNR" should be interpreted as the composite SNR of the crosslink and the downlink given by

$$1/(P/N)_{\text{composite return}} = 1/(P/N)_{\text{crosslink}} + 1/(P/N)_{\text{downlink}}.$$

To apply the curve to the Forward links the "Uplink SNR" parameter should be interpreted as the uplink SNR or (C/N) and the "Downlink SNR" ordinate should be interpreted as the composite SNR of the crosslink and the user link given by

$$1/(P/N)_{\text{composite forward}} = 1/(P/N)_{\text{crosslink}} + 1/(P/N)_{\text{user link}}$$

For the return links on TDRSS, the carrier to noise ratios on the user links are quite low according to Reference 2. Therefore, one would expect that a major contributor to the large ground equipment degradation is AM-to-PM degradation.

The other approach to mitigating AM-to-PM conversion is to provide amplitude linearizers in the system. Linearizers at 4 and 12 GHz have been successfully implemented in communication satellites with significant improvement in AM-to-AM and AM-to-PM performance. The most widely used types of linearizers are feed forward linearizers and predistortion linearizers. Of the two, the predistortion type is preferred for satellite applications because they can be realized with low power amplifiers and passive devices. If predistortion linearization is used for the bent pipe links on the channelized 60 GHz crosslink, the optimum place for the linearizer is in the lower frequency portion of the system before up converting to 60 GHz.

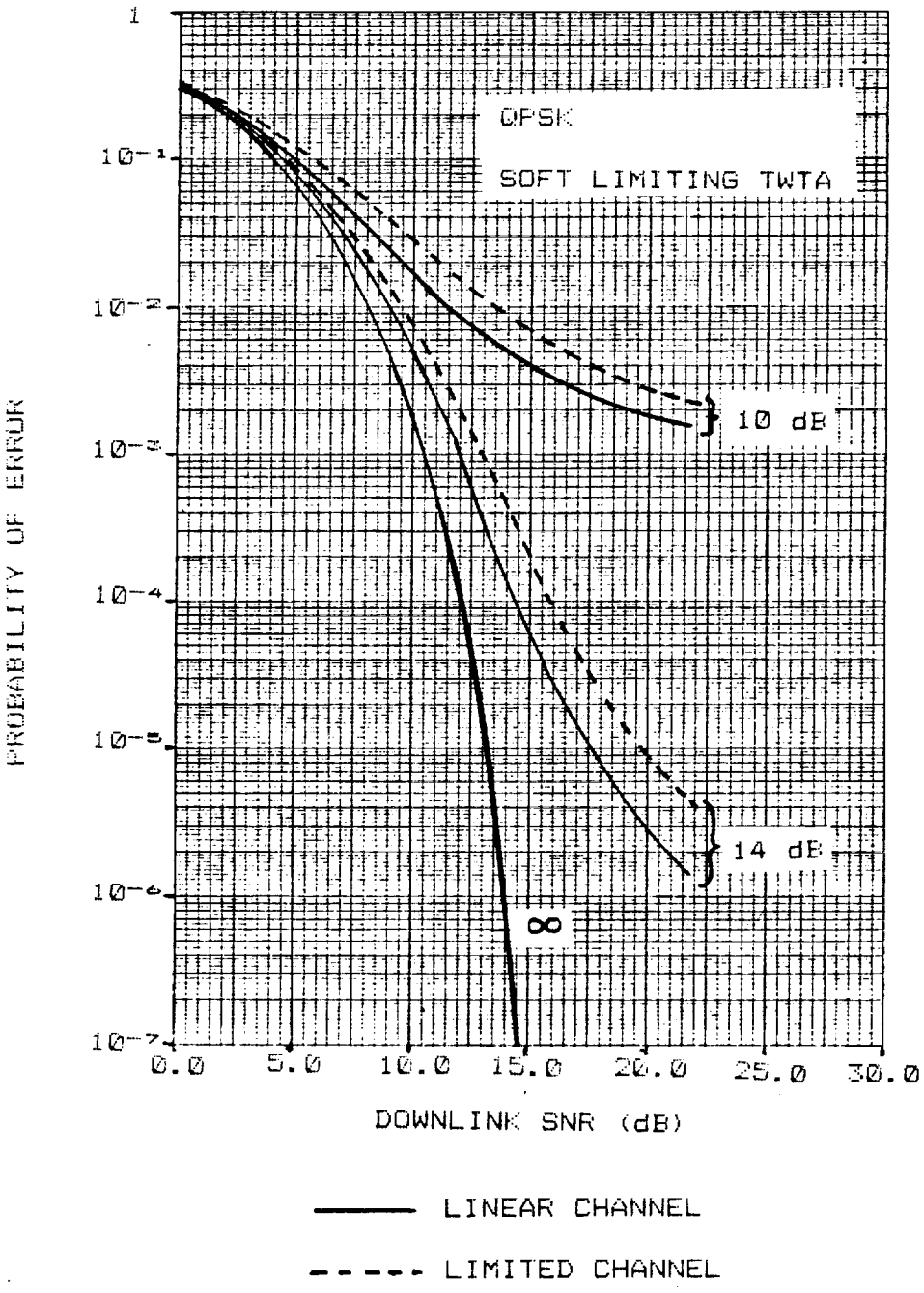

FIGURE A-22

SYMBOL ERROR PROBABILITY VS DOWNLINK SNR WITH UPLINK SNR AS A PARAMETER

Phase Jitter and Additive Thermal Noise Effects on Carrier Recovery

One of the sources of bit error rate degradation in coherent PSK systems is random phase errors in the carrier recovery loop. These phase errors are due to the cumulative effects of all noise entering the loop. Thermal noise is one contributor to the phase error; also every oscillator in the channel is a contributor. The phase stability performance of millimeter wave frequency sources is typically much worse than sources at lower frequencies since most millimeter wave oscillators are derived from a multiplication of lower frequency oscillators. The phase noise spectral density of the lower frequency oscillator is multiplied by the square of the multiplication factor. Thus, it is a good design practice to minimize as much as it is practical the number of up or down conversions in a channel.

To ensure that the channelized system will not suffer excessive degradation, calculations of phase errors in the carrier recovery loops were performed based on oscillator stabilities as reported in the hardware portion of the 60 GHz Intesatellite Study and on the signal to noise ratios as predicted in the link calculations in Section A.3 of this report.

Figure A-23 is a simplified diagram of a modulate/demodulate link used for phase noise calculations. The carrier recovery loop of the demodulator has been modeled as having a fourth power loop rather than a dual Costa loop. The contributors to phase noise of this link are:

Source phase jitter --this is phase jitter originating at the 60 GHz transmit source which is not reduced by improving the link signal to noise ratio.

Down converter phase jitter --this is phase jitter originating at the L.O. of the down converter and is directly added to the signal phase. Like the source phase jitter this jitter is not reduced by improving the link signal to noise ratio.

Demodulator VCO phase jitter --this is phase jitter originating at the VCO in the carrier recovery loop of the QPSK demodulator. This jitter is not reduced by improving the link signal to noise ratio.

Additive thermal noise --this is noise at the input to the carrier recovery loop. The effects of this noise can be reduced by increasing the signal to noise ratio in the loop.

The phase jitter power spectral density of the source was assumed to be as shown in Figure A-24 (Ref 3). This data is presented in the non-channelized portion of this study. The phase jitter power spectral density of the local oscillator in the down converter and the VCO in the demodulator are assumed to be the same as the source except scaled in frequency. In other words, when multiplication or division by N of an oscillator occurs then the phase noise spectral density is multiplied or divided by N^2.

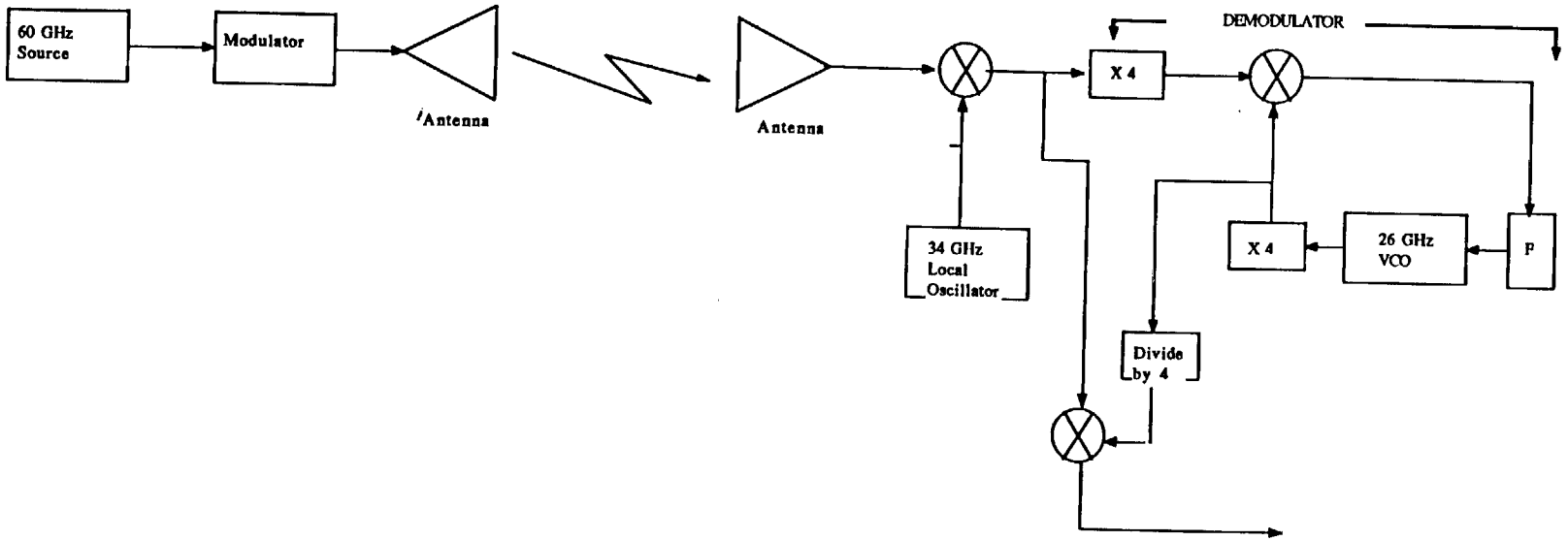

Figure A-23

MOD/DEMOD LINK MODEL USED FOR PHASE NOISE ANALYSIS

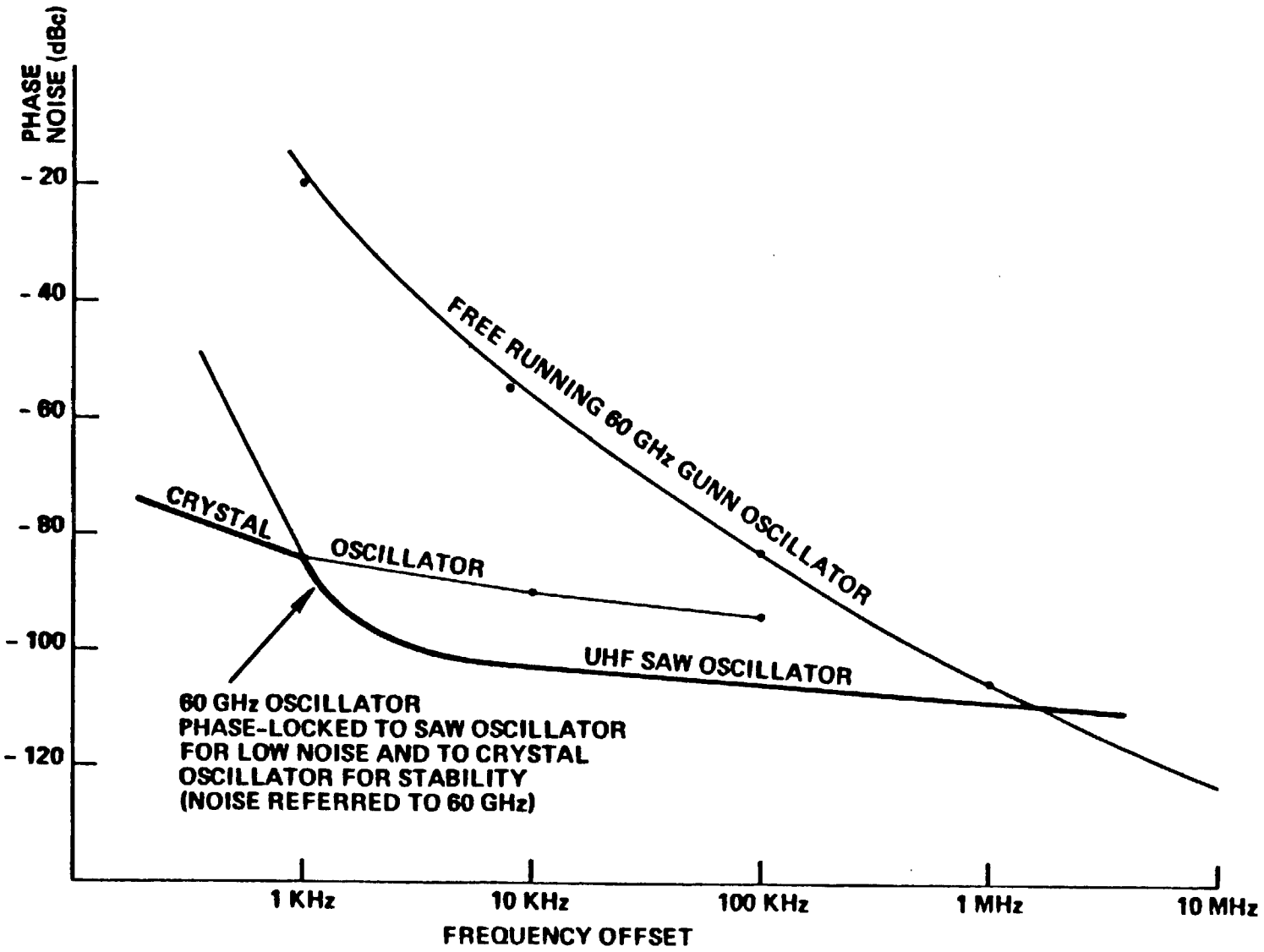
PHASE NOISE (dBc)
- 20
- 40
- 60
- 80
- 100
- 120
FREE RUNNING 60 GHz GUNN OSCILLATOR
CRYSTAL
OSCILLATOR
UHF SAW OSCILLATOR
60 GHz OSCILLATOR
PHASE-LOCKED TO SAW OSCILLATOR
FOR LOW NOISE AND TO CRYSTAL
OSCILLATOR FOR STABILITY
(NOISE REFERRED TO 60 GHz)
1 KHz
10 KHz
100 KHz
1 MHz
10 MHz
FREQUENCY OFFSET

Figure A-24

The probability of bit errors in QPSK transmission due to random phase errors has been computed (Ref 3) and is shown graphically in Figure A-25. The parameter σ^2_e is the total phase error variance in the carrier recovery loop. As previously mentioned, this variance is the sum of the variances attributable to each individual source,

$$\sigma^2_e = \sigma^2_{\text{thermal}} + \sigma^2_{\text{source}} + \sigma^2_{\text{down converter}} + \sigma^2_{\text{VCO}}$$

The phase error variance in the carrier recovery loop due to additive thermal noise is a function of the signal to noise ratio in the loop:

$$\sigma^2_{\text{thermal, } 4\omega_c} = 1/\text{SNR}_{\text{PLL}}$$

The $4\omega_c$ in the subscript denotes the variance in the loop at 4 times the carrier frequency; the variance in the recovered carrier is thus

$$\sigma^2_{\text{thermal}} = (1/4)^2 \sigma^2_{\text{thermal, } 4\omega_c} = 1/16\, \sigma^2_{\text{thermal, } 4\omega_c}$$

The signal to noise ratio was calculated from

$$\text{SNR}_{\text{PLL}} = \mathcal{B}\ (E_b/N_o)$$

where $\mathcal{B}$ is given by Spilker (Ref 4) as

$$\mathcal{B} = (W/B_n)/(14.1 + 55.5(N_o/E_b) + 61.5(N_o/E_b)^2 + 14.02(N_o/E_b)^3)$$

for the condition that TW = 2 where T is the symbol period, W is the bandwidth of the noise entering the fourth power multiplier, and B_n is the single sided loop bandwidth.

The phase jitter on the carrier due to the transmitting source will be partially tracked out by the carrier recovery loop. However, the portion of the phase noise spectrum that falls outside the loop bandwidth does contribute to the tracking error. The phase error variance due to the source jitter is then

$$\sigma^2_{\text{source}} = 2\int_0^\infty G_{\phi,s}(f)\,|1-H(f)|^2 df$$

where $G_{\phi,s}(f)$ is the single-sided phase jitter power spectral density of the source oscillator and H(f) is the closed loop transfer function of the carrier recovery loop.

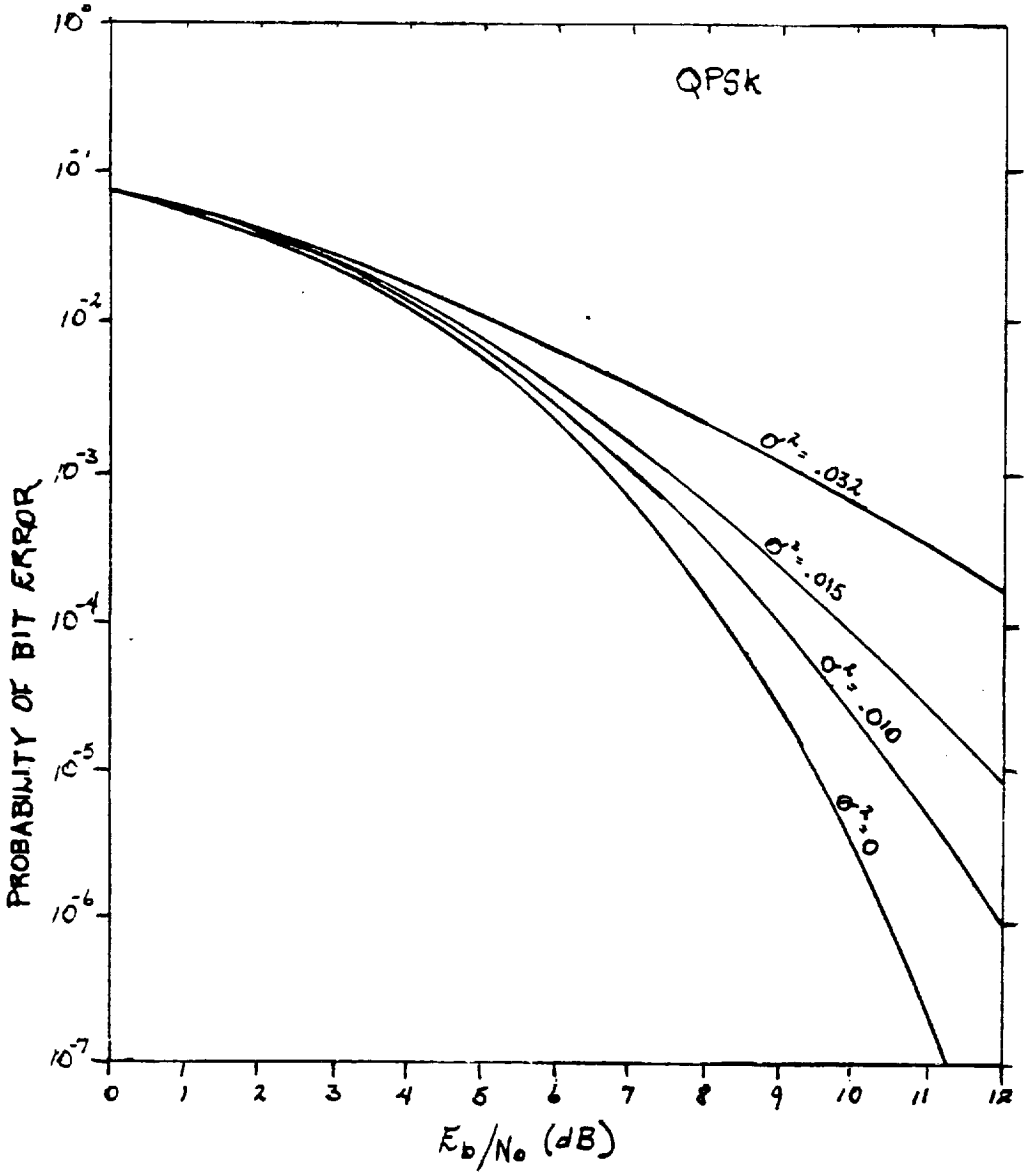

Figure A-25

Probability of QPSK Bit Error as a Function of E_b/N_o in the Presence of Phase Errors due to Partially Coherent Carrier Recovery

The phase jitter due to the down converter is also partially tracked out by the carrier recovery loop leaving a phase error variance of

$$\sigma^2_{\text{down converter}} = 2\int_0^\infty G_{\phi,D}(f)\,|1-H(f)|^2 df$$

where $G_{\phi,D}(f)$ is the single-sided phase jitter power spectral density of the local oscillator in the down converter.

The phase error variance due to the VCO is then

$$\sigma^2_{VCO} = 2\int_0^\infty G_{\phi,VCO}(f)\,|1-H(f)|^2 df$$

where $G_{\phi,VCO}$ is the single-sided phase jitter power spectral density of the VCO in the demodulator. The phase error variances that were just discussed refer to the phase error between the received carrier and the reference frequency obtained by dividing the frequency in the loop by 4. The phase error in the loop has a mean value that is 16 times larger.

An analysis of the phase error variance was performed using the link model shown in Figure A-24 and the phase jitter power spectral density of Figure A-25. The analytical model chosen for the carrier recovery loop was a second order phase-locked loop with a damping factor of 0.707 for which the loop tracking error is

$$|1-H(f)|^2 = (f/f_n)^4/(1 + (f/f_n)^4)$$

where f_n is the natural frequency of the loop which is related to the single-sided loop bandwidth by

$$B_n = 0.53 f_n/2\pi.$$

Analysis of the 55.02 Mbps, 100.51 Mbps, and 300 Mbps Mod/Demod links was performed using the E_b/N_o values determined from the link calculations and the IF bandwidth was determined from the inter-symbol interference analysis. The phase error analysis determined the phase error variance, σ^2_e, as a function of the recovery loop's single-sided noise bandwidth. Plots of the phase error variances as a function of single-sided loop bandwidth are shown in Figures A-26, A-27, and A-28.

It can be seen from the plots that if the bandwidth of the carrier recovery loop is properly chosen the phase error variance is less than 10^{-3} in all three cases. Figure A-25 shows the probability of bit error as a function of E_b/N_o with phase error variance as a parameter. From Figure A-25 it can be seen that the small phase error variances computed for the Mod/Demod links cause negligible BER degradation.

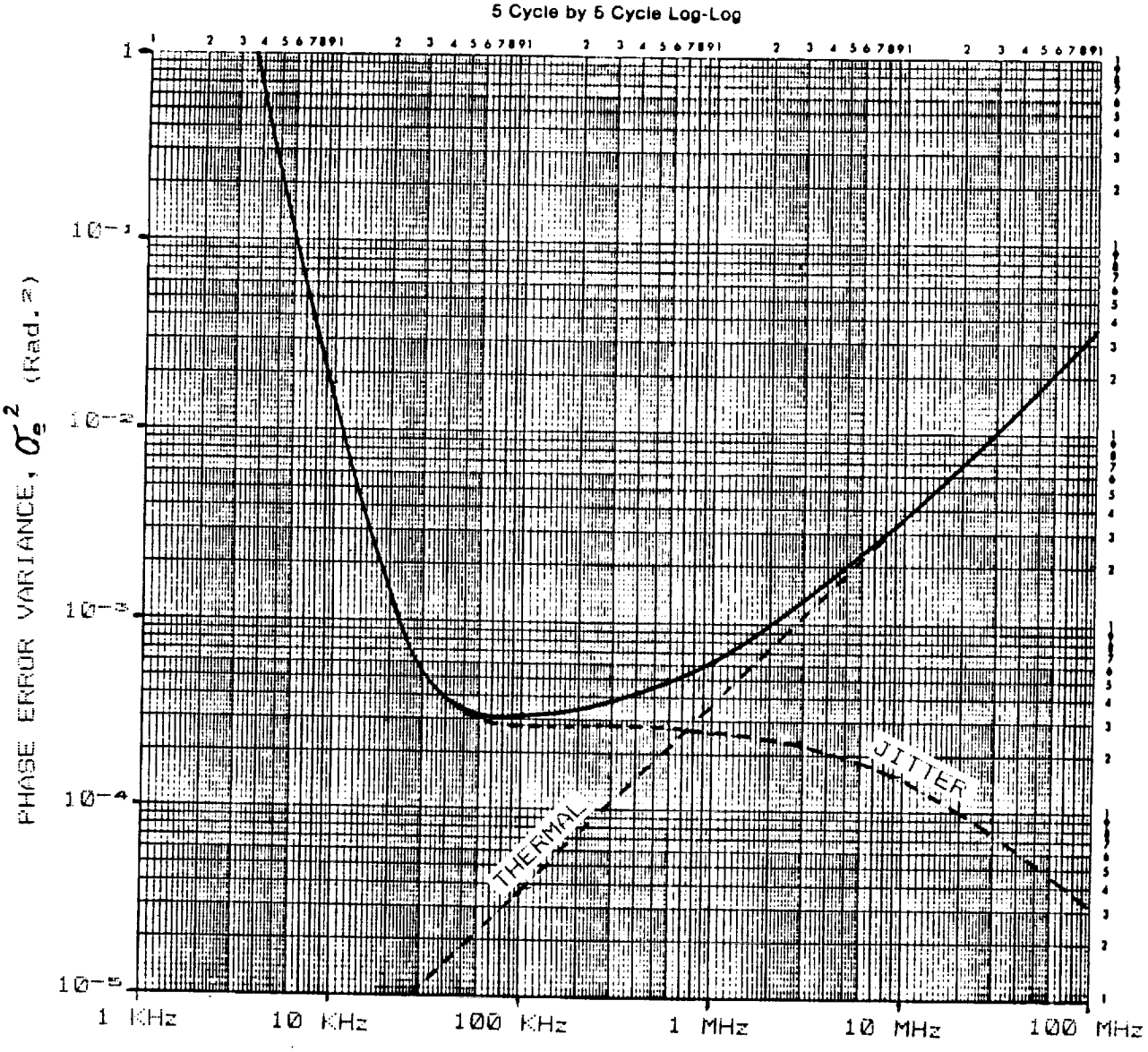

DATA RATE: 55.02 MBPS

E_b/N_0= 16.5 dB

IF BANDWIDTH: 60.1 MHz

Figure A-26

ORIGINAL PAGE IS
OF POOR QUALITY

PHASE ERROR VARIANCE DUE TO NOISE
IN THE QPSK CARRIER RECOVERY LOOP

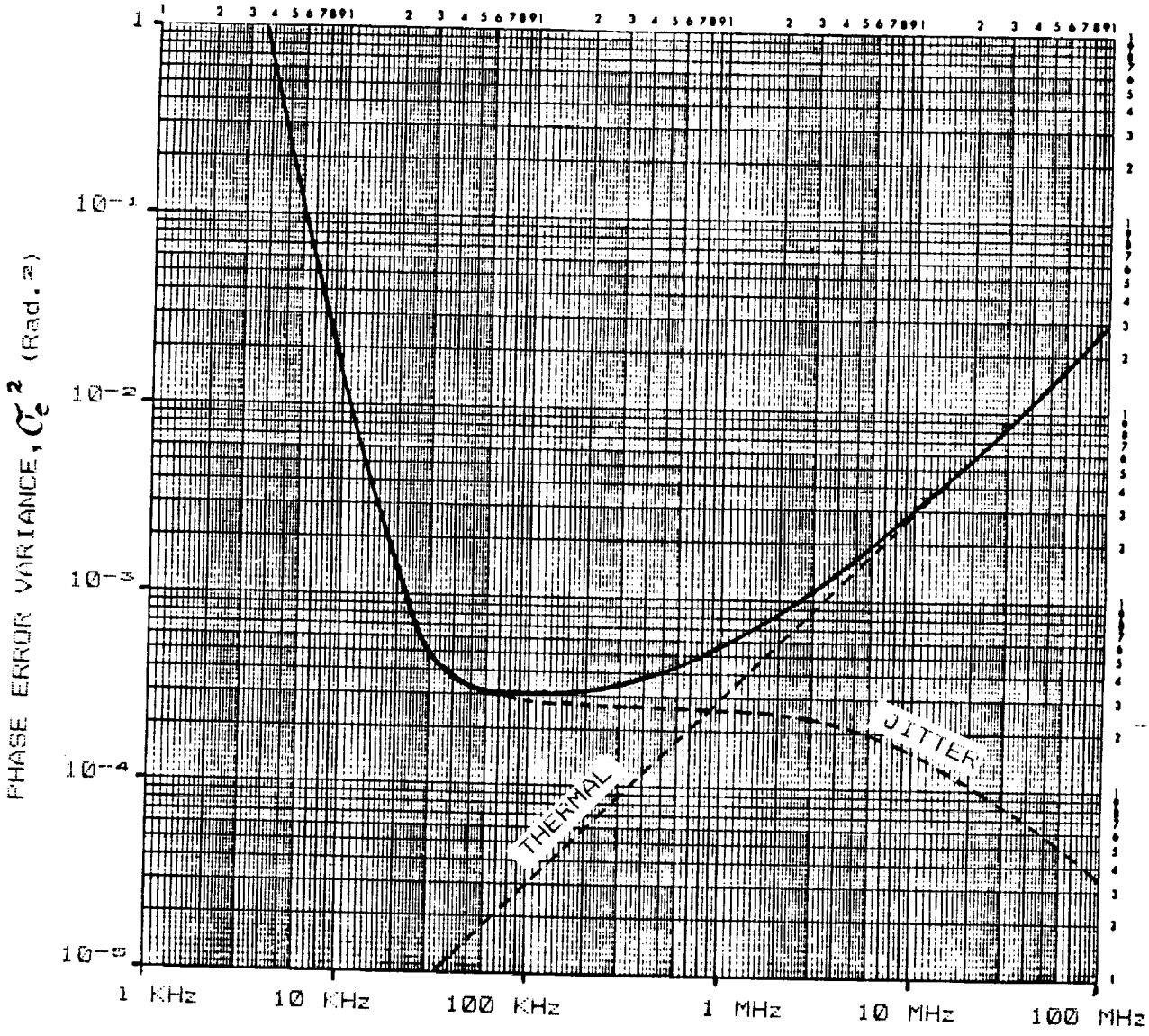

DATA RATE: 100.51 MBPS

E_b/N_0= 14.98 dB

IF BANDWIDTH: 109 MHz

ORIGINAL PAGE IS
OF POOR QUALITY

Figure A-27

PHASE ERROR VARIANCE DUE TO NOISE
IN THE QPSK CARRIER RECOVERY LOOP

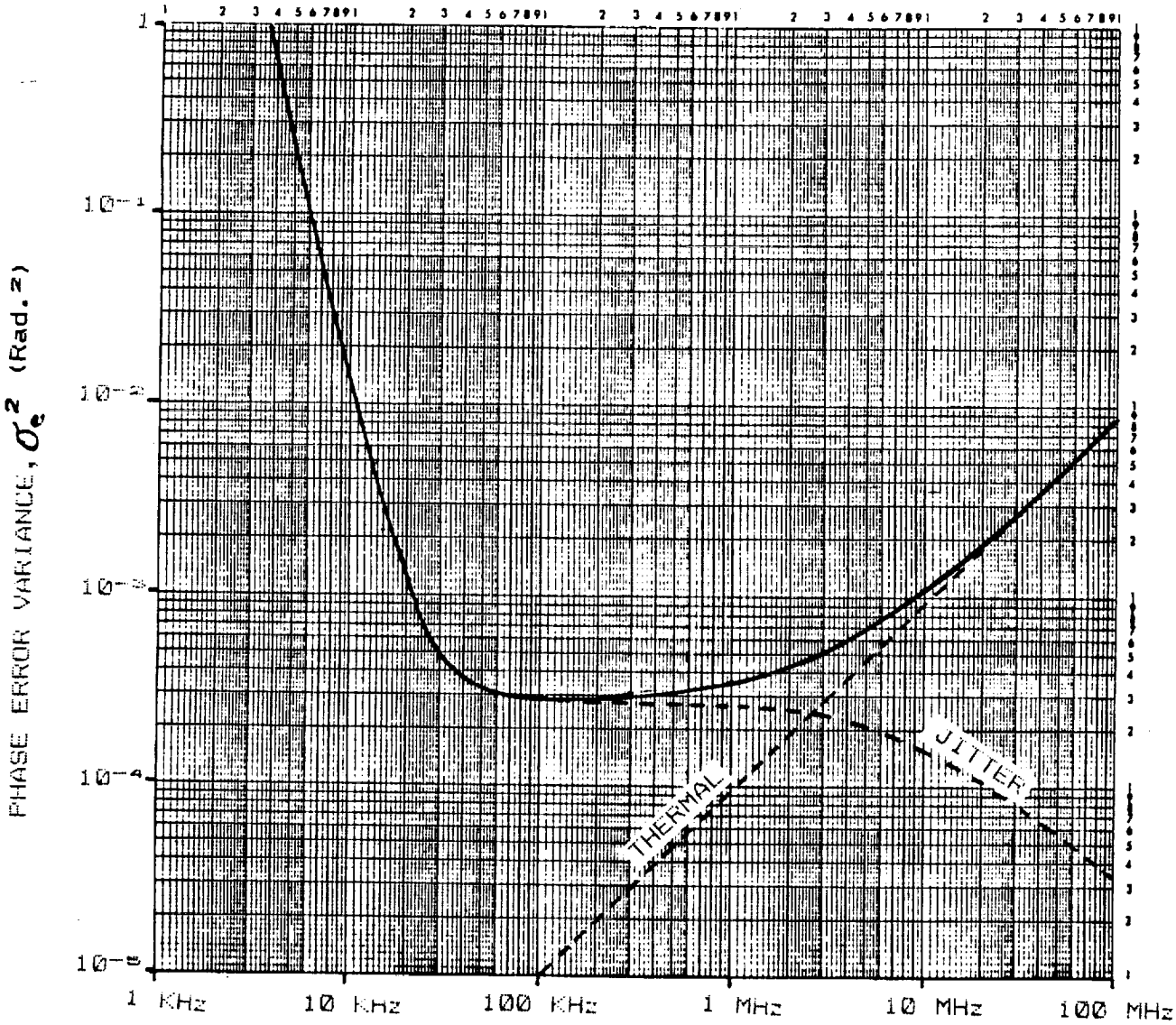

DATA RATE: 300 MBPS

E_b/N_0= 15.05 dB

IF BANDWIDTH: 328 MHz

ORIGINAL PAGE IS
OF POOR QUALITY

Figure A-28

PHASE ERROR VARIANCE DUE TO NOISE
IN THE QPSK CARRIER RECOVERY LOOP

A.6.0 RELIABILITY

A detailed reliability assessment of the channelized 60 GHz crosslink system has been performed on a link-by-link basis. A baseline redundancy design has been recommended. Appendix A to this addendum contains the reliability report.

A.7.0 POWER, WEIGHT AND SIZE

Estimates of the equipment power, weight and size have been made based on similar space qualified hardware. Tables A-4 and A-5 tabulate the physical characteristics for the frontside and the backside satellite communication equipment as shown in the block diagrams of Figures A-4 and A-5. Since the TDAS satellites are to be identical and interchangeable, the same equipment will be in place on both spacecrat but not all will be operating. Taking advantage of commonalities, the weight of the crosslink equipment will be 592.8 pounds. The satellite in the frontside orbital position will consume 722 watts of DC power, the one in the backside position will use 914 watts.

A.8.0 3 VS. 5 WSA CONSIDERATIONS

The channelized 60 GHz intersatellite crosslink system presented in this report was sized to accommodate five 60 GHz WSA 300 Mbps mod/demod return links plus a number of other links as detailed in Table A-3. If the number of WSA channels is reduced to three, there will be some impact on the crosslink system. First of all the deletion of two of the fourteen 300 MHz channels relieves some of the spectrum crowding at 60 GHz. This would permit increasing the guard band between channels, thereby simplifying the RF multiplexer design and reducing the multiplexer insertion loss. Analysis of the multiplexer shows that the insertion loss would only improve from 1.6 dB to 1.4 dB. The most significant impact will be in the reduction in weight and power. The weight of the GEO to GEO crosslink equipment will be reduced by an estimated 28.4 pounds, 16.8 pounds of frontside equipment and 11.6 pounds backside equipment. The power consumption is reduced by an estimated 66 watts on the frontside and 102 watts on the backside. These reductions in weight and power are in addition to the reductions that will be realized by eliminating two of the GEO-LEO communication packages.

60 GHZ CHANNELIZED CROSSLINK (GEO-GEO)

POWER, WEIGHT AND SIZE

FRONTSIDE SATELLITE

EQUIPMENT	QNTY	WEIGHT LB, EA	POWER W	SIZE " x " x "	REDUN-DANCY	TOTAL WEIGHT	TOTAL POWER
RETURN LINKS							
Low Noise Amplifier	11	0.3	3	1 x 3 x 0.75	10	6.3	33
Down Converter	10	5	24	5 x 4 x 2	8	85.0	240
Demodulator	9	3	6	3 x 4 x 2	8	51.0	54
Four Channel Down Converter	1	13	30	6 x 4 x 2	1	26.0	30
RF Demultiplexer	1	1.5	-	8 x 1 x 1	-	1.5	-
FORWARD LINKS							
60 GHz Modulator and Source	1	5	24	5 x 4 x 2	1	10.0	24
Power Amp (1 W)	1	0.5	11	4 x 2 x 1	1	1.0	11
Power Amp (0.025 W)	2	0.3	0.3	3.3 x 2 x 1	2	1.2	0.6
Power Amp (2 W)	2	0.7	22	10 x 5 x 1.5	2	2.0	44
Power Amp (0.1 W)	1	0.3	1	3.3 x 2 x 1	1	0.6	1
Up Converter	5	5	24	5 x 4 x 2	5	50.0	120
Power Combiner	1	0.7	-	8 x 1 x 1	-	0.7	-
Bandpass Filter	1	0.1	-	2 x 1 x 1	-	0.1	-
COMMON							
Feed Assembly	1	3.5	-	4 x 4 x 18	-	3.5	-
Antenna (3.2 m)	1	60.5	-	126 x 126 x 35	-	60.5	-
Gimbal Subsystem	1	28	9	14 x 13.5 x 11	-	28.0	9
Gimbal Drive Elec	1	5	6	8.5 x 2.6 x 5.7	1	10.0	6
Acquisition & Tracking Receiver	1	1.2	4	3 x 6 x 2	1	2.4	4
Antenna Controller	6	0.5	0.1	4 x 8 x 0.5	12	9.0	0.6
Antenna Control Microprocessor	1	0.5	0.4	4 x 8 x 0.5	2	1.5	0.4
DC/DC Converter	1	4	144.4	8 x 12 x 8	2	12.0	144.4

Table A-4

TOTAL WEIGHT: 234.1 lbs (single string)

373.1 lbs (with redundancy)

TOTAL POWER: 722 watts

60 GHZ CHANNELIZED CROSSLINK (GEO-GEO)

POWER, WEIGHT AND SIZE

BACKSIDE SATELLITE

EQUIPMENT	QNTY	WEIGHT LB, EA	POWER W	SIZE " x " x "	REDUN-DANCY	TOTAL WEIGHT	TOTAL POWER
RETURN LINKS							
60 GHz Modulator and Source	8	5	24	5 x 4 x 2	8	80.0	216
Power Amp (2.5 W)	8	0.7	27	10 x 5 x 1.5	8	11.2	216
Power Amp (1 W)	3	0.5	11	4 x 2 x 1	3	3.0	33
Power Amp (4 W)	2	0.8	43	10 x 5 x 1.5	2	3.6	86
Power Amp (0.1 W)	1	0.3	1	3.3 x 2 x 1	1	0.6	1
Up Converter	5	5	24	5 x 4 x 2	5	50.0	120
Power Combiner	1	0.5	-	8 x 1 x 1	-	0.5	-
RF Multiplexer	1	1.5	-	8 x 1 x 1	-	1.5	-
FORWARD LINKS							
Low Noise Amplifier	1	0.8	3	1 x 3 x 0.75	1	0.6	3
Bandpass Filter	1	0.1	-	2 x 1 x 1	-	0.1	-
Six Channel Down Converter	1	15	30	8 x 4 x 2	1	30.0	30
IF Demodulator	1	3	6	3 x 4 x 2	1	6.0	6
COMMON							
Feed Assembly	1	3.5	-	4 x 4 x 10	-	3.5	-
Antenna (3.2 m)	1	60.5	-	120 x 120 x 35	-	88.5	-
Gimbal Subsystem	1	20	8	14 x 13.5 x 11	-	28.0	8
Gimbal Drive Elec	1	5	6	8.5 x 2.8 x 5.7	1	10.0	6
Acquisition & Tracking Receiver	1	1.2	4	3 x 8 x 2	1	2.4	4
Antenna Controller	8	0.5	0.1	4 x 8 x 0.5	12	8.0	0.8
Antenna Control Microprocessor	1	0.5	0.4	4 x 8 x 0.5	2	1.5	0.4
DC/DC Converter	1	4	183	10 x 12 x 8	2	12.0	183

Table A-5

TOTAL WEIGHT: 205.3 lbs (single string)

346.6 lbs (with redundancy)

TOTAL POWER: 914 watts

A.9.0 SUMMARY

A system concept has been presented that will support a combination of mod/demod links and bent pipe links between two geostationary satellites at 60 GHz. The concept was used as a baseline to size the equipment, to analyse the link performance, and to identify technology advancements needed to meet the communication requirements. The system concept that has evolved appears quite feasible in the near term if 60 GHz technology continues to develop. Using 3 meter antennas on both satellites, the largest 60 GHz power amplifier required is a 4 watt unit. Although an amplifier with this much power has not been reported, it is possible even with today's technology to develop such an amplifier. Most of the other links require considerably less power. Low noise amplifiers with 3.5 dB noise figures have been assumed for receive preamplifiers. This is based on technology projections for HEMT devices in the 1989 time frame. Even if this technology goal is not achieved, the system concept can still be realized by re-allocating equipment performance within limits that are practical, such as increasing antenna gain, increasing power amplifier output, etc. The antenna concepts used are based on proven designs at lower frequencies. While considered a low risk technology, implementation of these designs at millimeter wave frequencies needs to be pursued in order to develop manufacturing techniques and structural/mechanical designs that can maintain the tolerances required at 60 GHz while operating in the space environment. The complex RF multiplexers required for the channelized system also need development. Preliminary anaysis of the filters involved has shown that they can be realized with reasonably low insertion loss and low channel distortion if projected filter Q's are realized. Development in filters is needed to realize better Q's at 60 GHz and to realize the tolerances and temperature stability required.

Consideration of AM-to-PM conversion has been presented in this report and was shown to be of significance in the bent-pipe links. Adequate link margin has been provided to overcome AM-to-PM degradation.

Phase noise analysis has been presented in detail for the mod/demand links. Based upon published oscillator phase noise performance, the system can be implemented with negligible phase noise degradation. This does not mean that phase noise can be neglected; however, with proper oscillator designs and carrier recovery loop bandwidths the effect can be minimal.

Reliability analysis has been performed on the crosslink system based on a high level of redundancy. Recommendations have been made to derate the IMPATT diodes in the power amplifiers. Concern over the availability of appropriate IMPATT diodes with sufficient reliability for a 10 year mission has been expressed. The need for a better reliability data base on IMPATT diodes is of the utmost importance.

REFERENCES:

1. P. Jain, T Huang, K. Woo, J. Omura, W. Lindsey, "Detection of Signals Through a Nonlinear Satellite Repeater", Proc. of the NTC (Dec. 1977).

2. "TDRSS Telecommunications Performance and Interface Document (TPID)", SE-09, 12 March 1984.

3. T. Parker, "SAW Controlled Oscillators", Microwave Journal, October 1978

4. S. Rhodes, "Performance of Offset-QPSK Communications with Partially Coherent Detection", Proc. of the NTC (1973).

5. J. Spilker, Digital Communications by Satellite (Englewood Cliffs, N.J.: (Englewood Cliffs, N.J.: Prentice-Hall 1977), p. 393.

APPENDIX A

ISL RELIABILITY

MAY 1986

1.0 **Reliability Prediction Assessment**

This section discusses the reliability assessment and results for the six intersatellite return and forward links considered in this report. The reliability models for the individual intersatellite links are provided in Figures 1 through 10. Models are shown for configurations with and without redundancy. The hardware items required for redundancy are shown outlined in the link models. Items shown in the link reliability models include the hardware elements between the multiplexers and the demultiplexers.

Although the antennas and feeds are shown in the link models, the drive mechanisms for the antennas are not shown. Figure 11 provides the reliability model for a possible antenna drive mechanism. Since the reliability results for the individual links are significantly affected by the reliability of the antenna drive mechanisms, reliability results are provided for each link with and without the antenna drive mechanisms. The antenna drive mechanism reliability assumes hardware redundancy both for the single thread and redundant link calculations. The reliability results for the links are summarized in Table 1.

Table 1
LINK RELIABILITY
P_S(10 years)

	Single Thread		**With Redundancy**	
Link Name	W/O Drive	W Drive*	W/O Drive	W Drive*
LSA Return	0.1430	0.1339	0.8962	0.8392
LSA Forward	0.7071	0.6622	0.9589	0.8980
WSA Return	0.6039	0.5655	0.9340	0.8746
WSA Forward	0.7071	0.6622	0.9589	0.8980
TT&C Return	0.7342	0.6875	0.9669	0.9054
TT&C Forward	0.7304	0.6840	0.9655	0.9041
SMA Return	0.6362	0.5958	0.9437	0.8837
SMA Forward	0.7071	0.6622	0.9589	0.8980
KSA Return	0.5979	0.5599	0.9228	0.8641
KSA Forward	0.6679	0.6255	0.9481	0.8878
SSA Return	0.7111	0.6659	0.9607	0.8996
SSA Forward	0.7294	0.6830	0.9642	0.9029

* Antenna drive mechanisms include redundant electronics (See 2.4).

1.1 Reliability Modeling Assumptions

The following reliability assumptions are incorporated in the link reliability models:

- High reliability parts and components in accordance with typical long life spacecraft.
- Part derating policies in accordance with MIL-STD-1547 and PPL-17 for a 10 year mission.
- 12 year design life for electronics and antenna drive mechanisms.
- Operating temperatures for assemblies typical of 3 axis spacecraft in geosynchronous orbit.
- Failure rates for piece parts in accordance with MIL-HDBK-217D, Notice 1.
- The reliability or probability of success for all items in the link models is determined by the exponential formula;

  $R(t) = e^{-\lambda t}$

  where λ = the hardware failure rate in failures per 10^9 hours
  and t = mission time (10 years for this assessment)

- The reliability of redundant items with spares in a standby unpowered configuration is determined using the following expression;

  $$R(t) = [\, P^m \Pi^x_{r=0} (rk + m)]/[x!\, k^x] \cdot \Sigma^x_{r=0} \{ [(-1)^r (r^x) P^{rk}]/[rk + m]\}$$

  where n = the total number of units
  m = number of required operating units
  x = n - m (the number of spare units)
  k = the portion of the active failure rate applicable to the standby unpowered units (10% for this assessment)
  $P = e^{-\lambda t}$

1.2 Considerations for Redundancy

Two for one redundancy (one operational unit(s) and a single nonoperational spare) is assumed for most equipment in the link models since this appears to be sufficient in achieving high reliability for a ten year mission. Higher levels of redundancy are required for the LSA Return Link because significantly more hardware items are required for this link. Six for three and five for three redundancy are assumed for selected equipment in the LSA Return Link (Figure 1).

It has been assumed for the redundancy shown in the link models that all redundant hardware items are dedicated to the links shown. In an actual flight configuration it is possible that redundant items may be shared between the various links to reduce hardware requirements while providing the necessary overall payload redundancy and sparing flexibility.

Two for one redundancy is shown in Figure 11 for the electronic portions of the antenna drive hardware, including the tracking & acquisition receivers, gimbal electronic circuitry, motor windings, optical encoders and modulator drivers. Because of the higher failure potential of the antenna processors and controllers, three for one redundancy is assumed for these items. Redundancy is not assumed for the antenna reflectors or structure, feed components, or the mechanical drive components. The cross-strapping shown for the antenna drive electronic assemblies is considered the most likely in terms of complexity, interfaces, and for meeting the requirements of a ten year mission. The estimated probability of success of a single antenna drive configuration (as shown in Figure 11 excluding the antenna and feed) is 0.9677 for 10 years. In a single link, two sets of antenna drive mechanisms are required for an overall antenna drive 10 year probability of success for each link of 0.9364.

The antenna drive reliability for each link can be increased somewhat by also incorporating three for one redundancy for the tracking & acquisition receivers. The 10 year probability of success would increase from 0.9364 for the baseline to 0.9567. At this time, three for one redundancy for the receivers is not assumed for the baseline because of the additional design complexities and interfacing problems that would result.

2.0 **Hardware Reliability**

The following sections provide the details for the reliability estimates of the hardware elements included in the link reliability models. The failure rates for the component items are derived from similar component designs on current programs, MIL-HDBK-217D estimates for piece parts, engineering estimates, or projections of achievable reliability for some items.

2.1 Power Amplifiers

The key hardware components in the link models are the power amplifiers. The failure rates for the power amplifiers are almost entirely dependent upon the achievable failure rates for the IMPATT diodes which are used in the designs. In this reliability assessment the power amplifiers are assumed to range in output power from 25MW to 4W. As shown in Table 2, one important consideration for maximizing overall payload reliability is to use power amplifiers with the lowest output power requirements (resulting in lower failure rates) which will provide the necessary signal to noise link margins. It is equally important to provide conservative power amplifier redundancy for the higher power applications (>1W) due to the uncertainity concerning IMPATT diode failure rates at 60 Ghz.

For modeling purposes, it is assumed that the IMPATT diodes required to provide lower output power are more reliable than those providing higher output power (0.5 to 1W each). The maximum failure rate assumed is 500 x 10^{-9} for the final high power stages of the power amplifiers. It is also assumed that degraded operation resulting from failure of one or more diodes is not feasible for the power amplifiers. The failure rates for the power amplifiers are derived in Table 2.

2.1.1 IMPATT Diode Reliability

As previously mentioned, power amplifier reliability is primarily dependent upon the failure rate of the IMPATT diodes used in the amplifiers. There are limited sources of information which provide failure rates for space flight qualified diodes. The best source for IMPATT diode failure rates is MIL-HDBK-217D, Notice 1. This document provides a

Table 2
Power Amplifier Failure Rates

Item	Item Failure Rate	n	Total Failure Rate
Mixer	100	1	100
Crystal Controlled Osc. (Temp controlled oven)	250	1	250
Isolator	5	3	15
Subtotal			365
25 to 100MW Amplifier			
1st stage (1 IMPATT)	150	1	150
Total			515
1W Amplifier			
1st stage (1 IMPATT)	500	1	500
Total			865
2 to 2.5W Amplifier			
1st stage (1 IMPATT)	150	1	150
2nd stage (2 IMPATTs)	1000	1	1000
Total			1515
4W Amplifier			
1st stage (1 IMPATT)	150	1	150
2nd stage (2 IMPATTs)	400	1	400
3rd stage (4 IMPATTs)	2000	1	2000
Total			2915

point estimate of 500 FITs (failures per 10^{-9} hours) per diode. The 217D data, however, is based on a small amount of available IMPATT diode reliability data. Unfortunately, the failure rate data given in 217D does not differentiate IMPATT diode failure rates for power ratings, application frequencies, or the nature and history of the technology.

Previous discussions with researchers and users of IMPATT diodes has uncovered no new substantial reliability data which would add to the

confidence in the failure rates assumptions for these devices in the ISL power amplifiers. It appears that 1) there is apparently no substantial work in progress to characterize failure rates for IMPATT diodes by the agencies contacted; 2) more definitive failure rate data on IMPATT diodes for the ISL applications does not appear to be forthcoming in the near future.

As a result of the reliability risks associated with using IMPATT diodes, which is attributed to this lack of reliability data, a conservative design approach is required in terms of redundancy for the power amplifiers in the ISL applications as well as derating of the IMPATT diodes in the amplifiers. Since failure rates are expected to be higher for the IMPATT diodes used in the higher power amplifiers, it is recommended that lower power amplifiers be used whenever possible even at the sacrifice of performance and link margins.

This writer has a concern over the effort underway to ensure that the appropriate IMPATT diodes with sufficient reliability (for a 10 year mission) will be available at the time the power amplifiers are required. A special and continuing effort is recommended to ensure that such devices will be available prior to the proposal efforts for procurement of spacecraft with interlink communication capabilities. To expect the appropriate IMPATT diodes to be available at a later date without directed efforts could adversely affect the reliability of the power amplifiers.

2.2 Uplink and Downlink RF Component Reliability

The basis for the failure rates for the modulators, up converters, down converters, demodulators, and tracking & acquisition receiver are shown in Table 3. A failure rate of 150 FITs has been assumed for the low noise amplifiers (LNA) which should be achievable even with 1986 technology. The failure rate shown for the downconverter is for a 1 channel downconverter. There is a slight increase in failure rate for each channel when 4 and 6 channel downconverters are used.

Table 3
RF Component Failure Rates

Item	Item Failure Rate	n	Total Failure Rate
Modulator			
V-Band oscillator			
Isolator	5	4	20
Power divider	10	2	20
Mixer	100	3	300
V-Band GUNN Osc.	600	1	600
Loop Filter	10	1	10
Bandpass filter	5	2	10
Amplifier	20	1	20
Lowpass filter	5	1	5
Correction amplifier	20	1	20
Multiplier	30	1	30
Divider	30	1	30
SAW VCO (UHF)	30	1	30
XTAL oscillator	50	1	50
Loop amplifier	20	1	20
Subtotal			1165
3db power divider	10	1	10
Biphase switch	130	2	260
3 db power combiner	10	1	10
Microstrip/WG transition	10	1	10
DC/DC converter	90	1	90
Total			1545
Upconverter or Downconverter			
V-Band oscillator	1165	1	1165
Mixer	100	1	100
DC/DC converter	90	1	90
Total			1355
Demodulator			
Mixer	100	5	500
Lowpass filter	5	4	20
Loop filter	20	1	20

Table 3 (Continued)

Item	Item Failure Rate	n	Total Failure Rate
Limiter	20	2	40
VCO	25	1	25
Summer	75	1	75
Sample/latch	50	2	100
Bandpass filter	5	1	5
$\tau/2$	30	2	60
PPL	60	1	60
Clock	100	1	100
DC/DC converter	90	1	90
Total			1095
Acquisition & Tracking Receiver			
Mixer	100	3	300
IF amp	103	2	206
Bandpass filter	5	1	5
AM detector	20	1	20
Lowpass filter	5	3	15
DC amp	20	1	20
LO.	400	1	400
Scan generator	200	1	200
Timing generator	250	1	250
Summer	75	1	75
Threshold logic	90	1	90
Demux	50	1	50
DC/DC converter	90	1	90
Total			1721

2.4 Antenna and Drive Mechanisms Reliability

Figure 11 provides the reliability model for the ISL antenna and antenna drive mechanisms. Redundancy is assumed for all electronics including the modulator drivers. The reliability model for a single thread configuration for this equipment is not shown in this report since it will not meet the requirements of a ten year mission. Due to the higher failure rates of the antenna processor and controller, three for one redundancy is assumed for this equipment to ensure adequate 10 year mission reliability.

The failure rate for the tracking and acquisition receiver is derived from Table 3. The failure rate for the gimbal drive electronics is the same as that used on the Intelsat V spacecraft which is based on a MIL-HDBK-217 piece part failure rate assessment using actual calculated stresses for each piece part. The failure rates for the antenna control processor and controller are estimates based on the assumptions in Table 4.

Table 4
Antenna Processor and Controller Failure Rates

Item	Item Failure Rate	n	Total Failure Rate
Antenna Control Processor			
Processor circuits	500	1	500
4Kx8 ROM	250	1	250
8Kx8 ROM	600	1	600
Interface circuits	150	6	900
DC/DC converter	90	1	90
Total			2340
Antenna Controller			
Processor circuits	500	1	500
4Kx8 ROM	250	1	250
8Kx8 RAM	600	1	600
Interface circuits	150	2	300
DC/DC converter	90	1	90
Total			1740

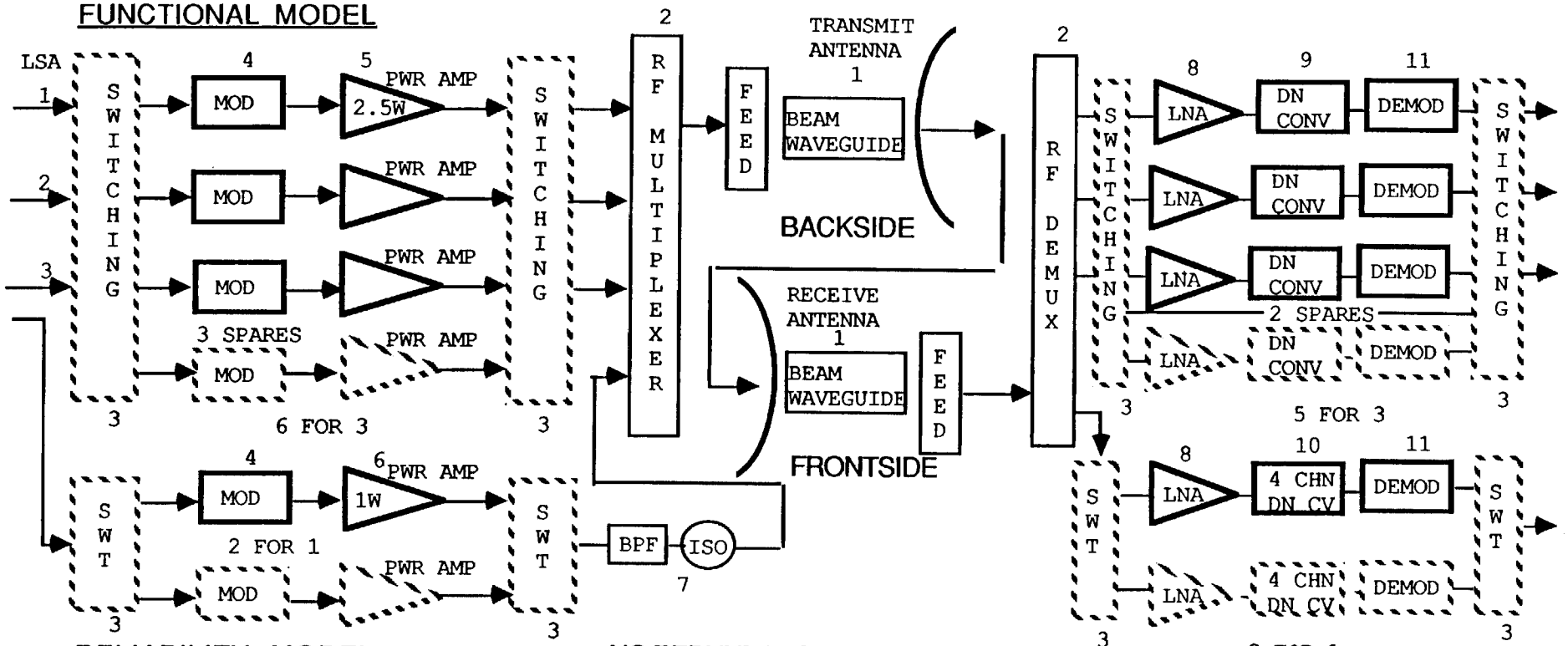

RELIABILITY MODEL

	F.R.
1. ANTENNA/BEAM WG/ FEED	28.5
2. MULTIPLEXER PORT	10
3. SWITCH PORT	5
4. MODULATOR	1545
5. 2.5W PWR AMP	1515
6. 1W PWR AMP	865
7. BPF/ISOLATOR	10
8. LNA	150
9. DOWN CONVERTER(1 CHN)	1355
10. DOWN CONVERTER(4 CHN)	1400
11. DEMODULATOR	1095

NO REDUNDANCY

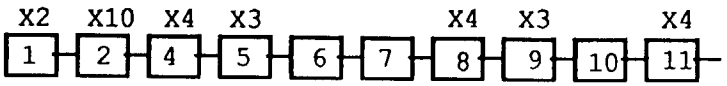

WITH REDUNDANCY

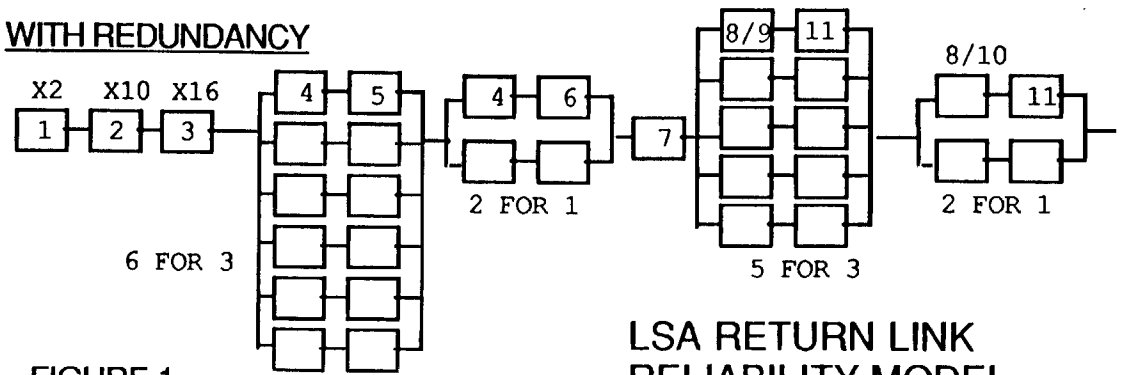

FIGURE 1

LSA RETURN LINK RELIABILITY MODEL

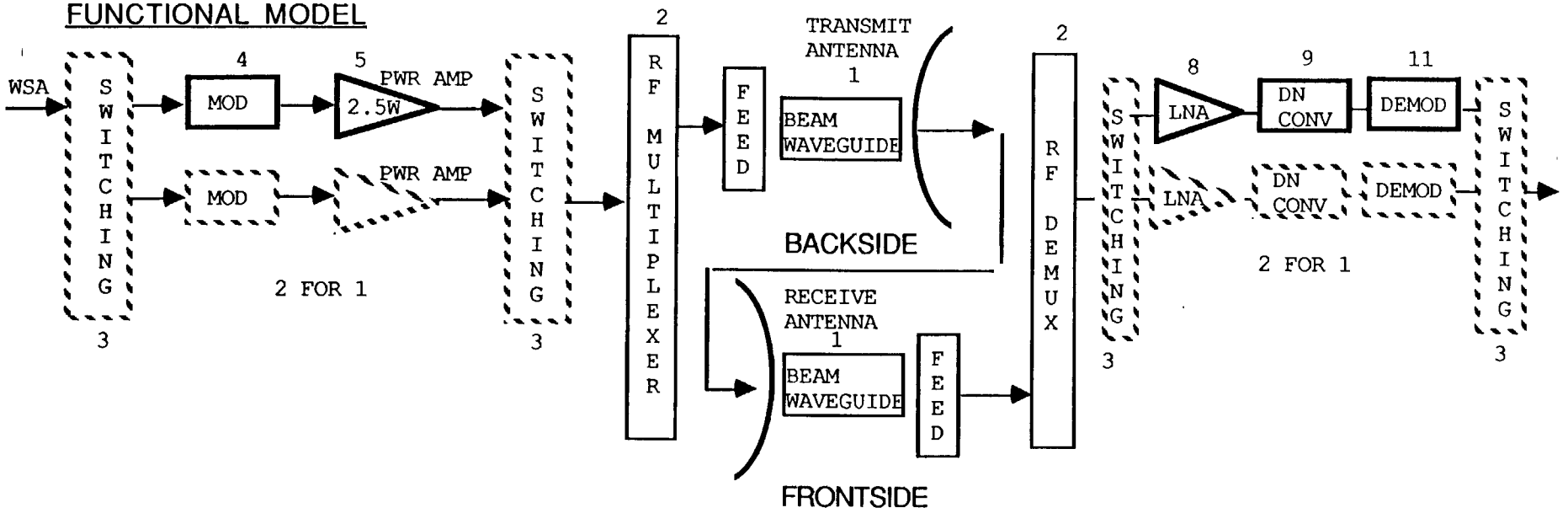

RELIABILITY MODEL

	F.R.
1. ANTENNA/BEAM WG/ FEED	28.5
2. MULTIPLEXER PORT	10
3. SWITCH PORT	5
4. MODULATOR	1545
5. 2.5W PWR AMP	1515
8. LNA	150
9. DOWN CONVERTER(1 CHN)	1355
11. DEMODULATOR	1095

NO REDUNDANCY

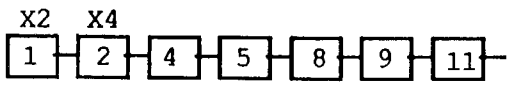

WITH REDUNDANCY

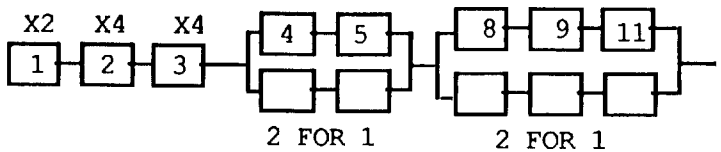

FIGURE 2

WSA RETURN LINK
RELIABILITY MODEL

FUNCTIONAL MODEL

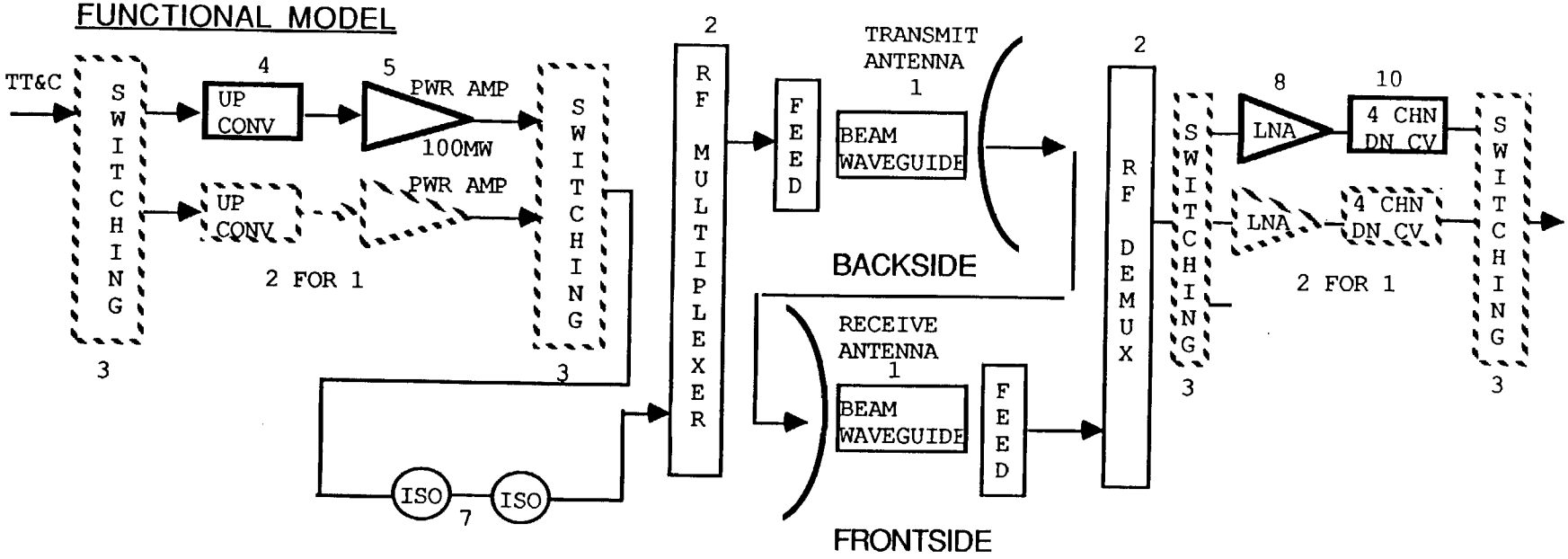

RELIABILITY MODEL

	F.R.
1. ANTENNA/BEAM WG/ FEED	28.5
2. MULTIPLEXER PORT	10
3. SWITCH PORT	5
4. UP CONVERTER	1355
5. 100MW PWR AMP	515
7. ISOLATOR(2)	10
8. LNA	150
10. DOWN CONVERTER(4 CHN)	1400

NO REDUNDANCY

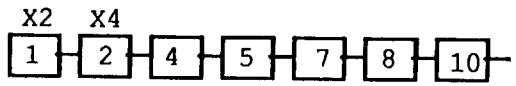

WITH REDUNDANCY

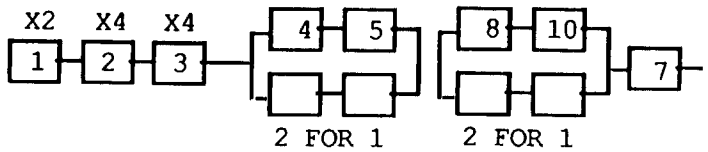

FIGURE 3

TT&C RETURN LINK RELIABILITY MODEL

FUNCTIONAL MODEL

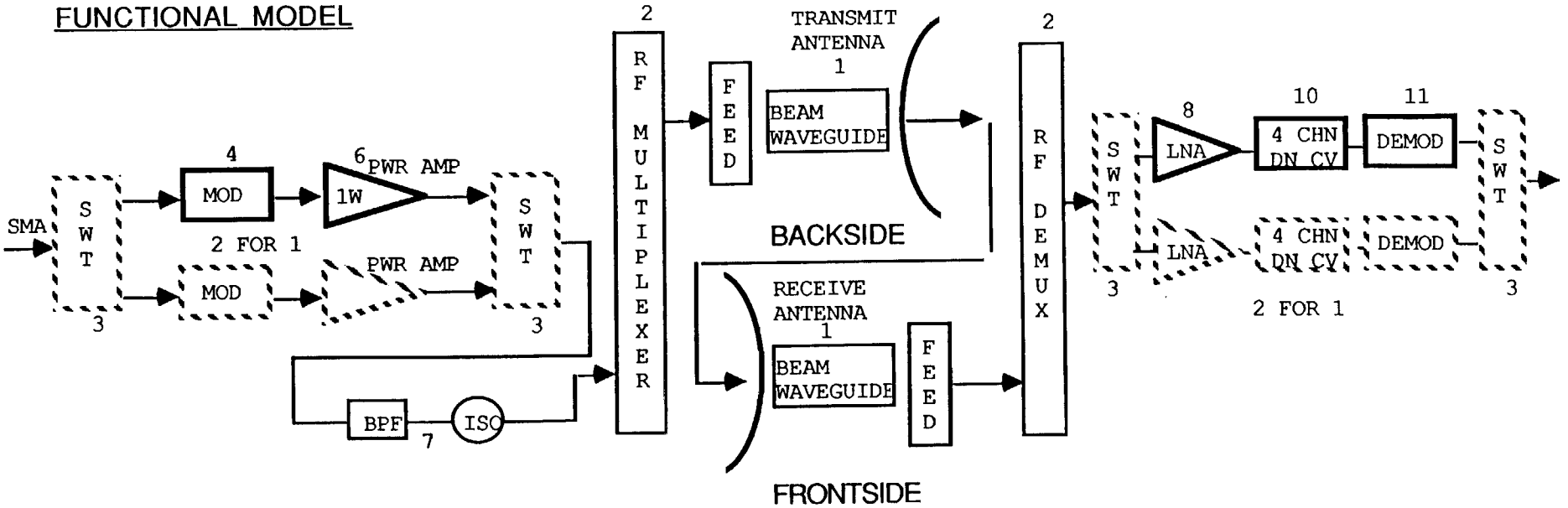

RELIABILITY MODEL

	F.R.
1. ANTENNA/BEAM WG/ FEED	28.5
2. MULTIPLEXER PORT	10
3. SWITCH PORT	5
4. MODULATOR	1545
6. 1W PWR AMP	865
7. BPF/ISOLATOR	10
8. LNA	150
10. DOWN CONVERTER(4 CHN)	1400
11. DEMODULATOR	1095

NO REDUNDANCY

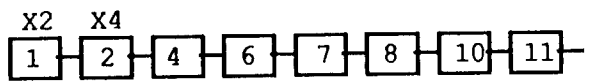

WITH REDUNDANCY

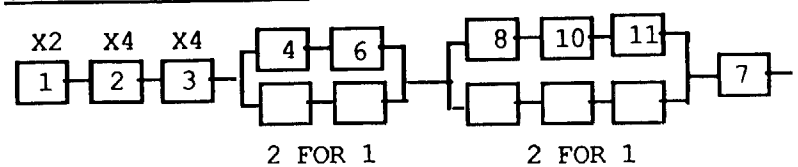

FIGURE 4

SMA RETURN LINK
RELIABILITY MODEL

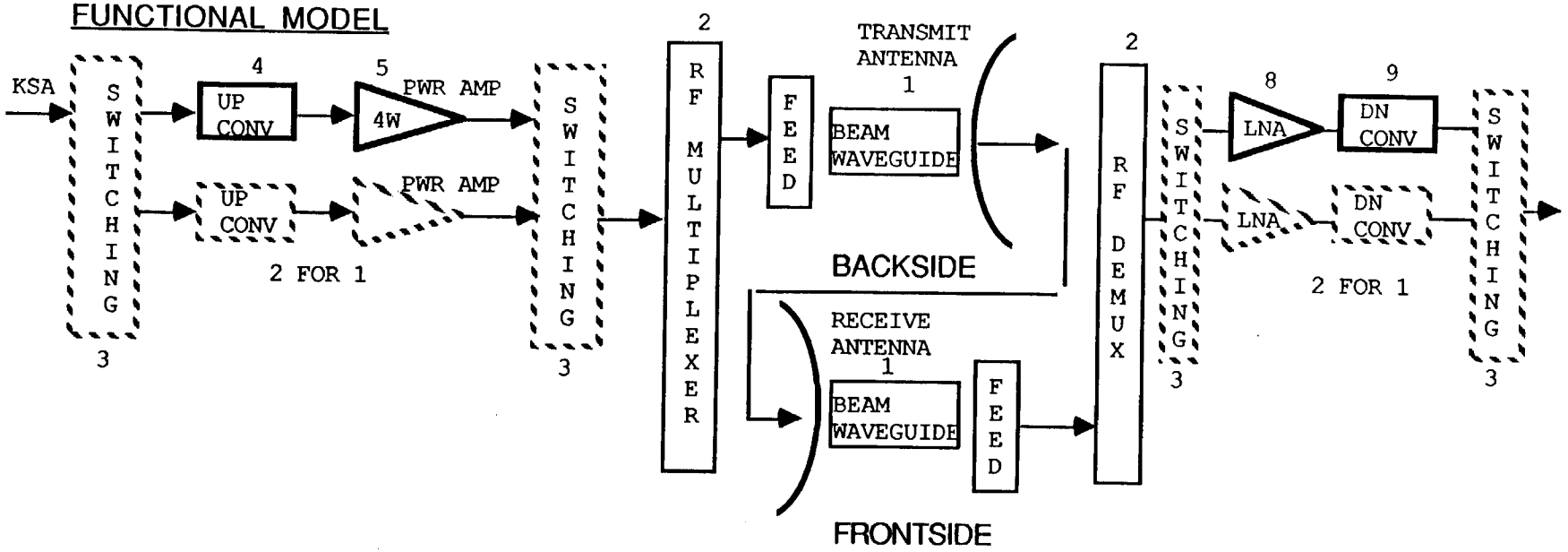

RELIABILITY MODEL

	F.R.
1. ANTENNA/BEAM WG/ FEED	28.5
2. MULTIPLEXER PORT	10
3. SWITCH PORT	5
4. UP CONVERTER	1355
5. 4W PWR AMP	2915
8. LNA	150
9. DOWN CONVERTER(1 CHN)	1355

NO REDUNDANCY

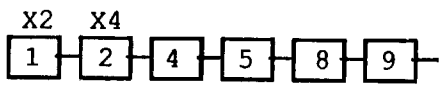

WITH REDUNDANCY

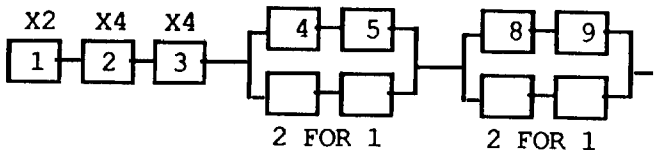

FIGURE 5

KSA RETURN LINK RELIABILITY MODEL

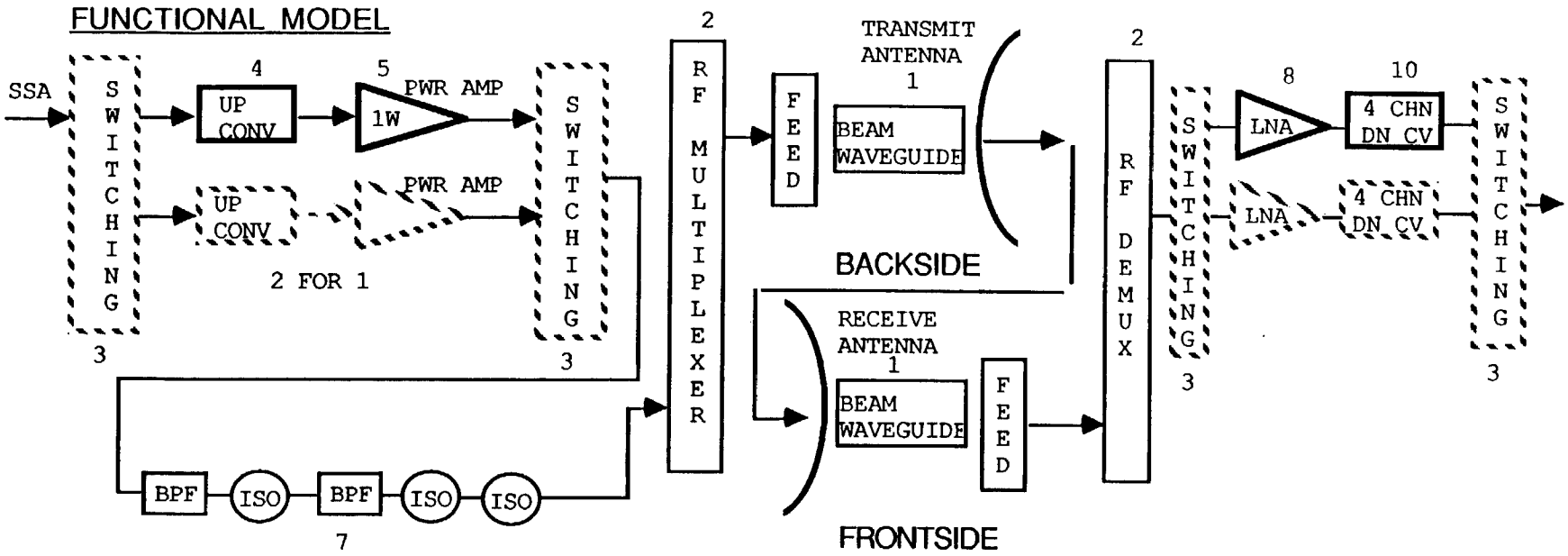

RELIABILITY MODEL

	F.R.
1. ANTENNA/BEAM WG/ FEED	28.5
2. MULTIPLEXER PORT	10
3. SWITCH PORT	5
4. UP CONVERTER	1355
5. 1W PWR AMP	865
7. BPF(2)/ISOLATOR(3)	25
8. LNA	150
10. DOWN CONVERTER(4 CHN)	1400

NO REDUNDANCY

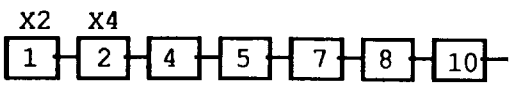

WITH REDUNDANCY

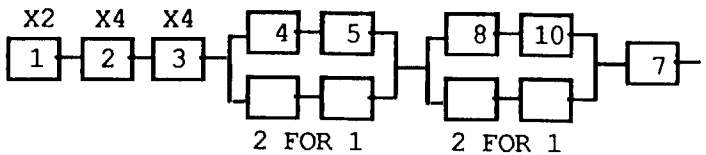

FIGURE 6

SSA RETURN LINK
RELIABILITY MODEL

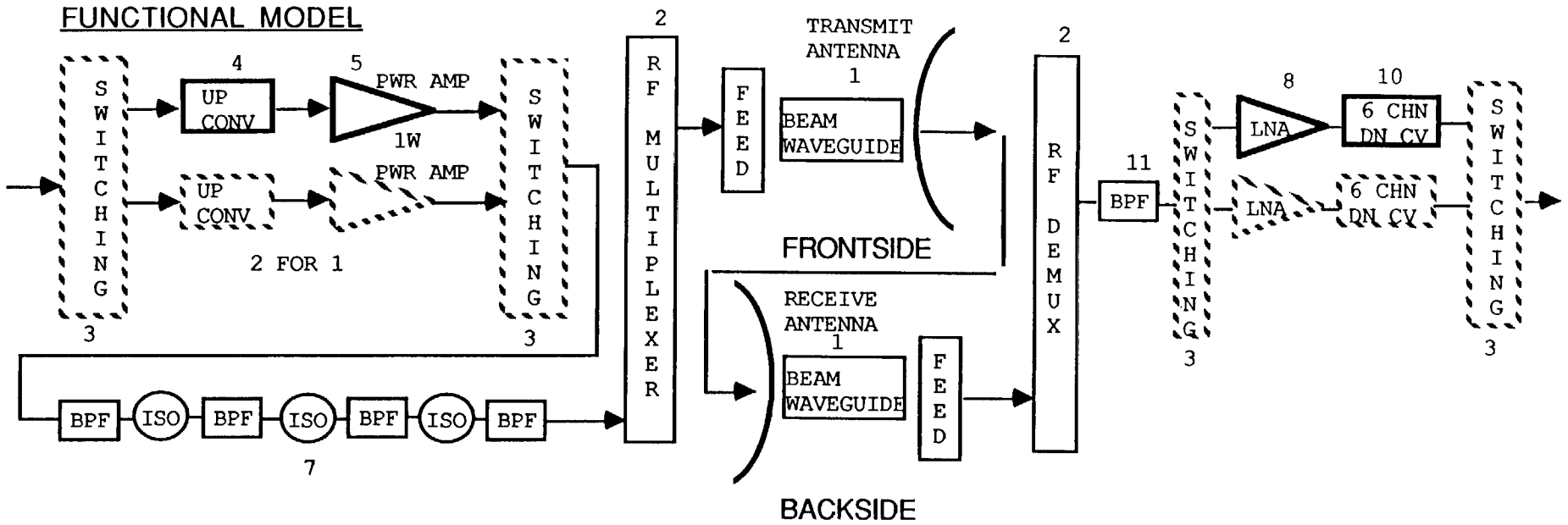

RELIABILITY MODEL

	F.R.
1. ANTENNA/BEAM WG/ FEED	28.5
2. MULTIPLEXER PORT	10
3. SWITCH PORT	5
4. UP CONVERTER	1355
5. 1W PWR AMP	865
7. BPF(4)/ISOLATOR(3)	35
8. LNA	150
10. DOWN CONVERTER(6 CHN)	1450
11. BPF	5

NO REDUNDANCY

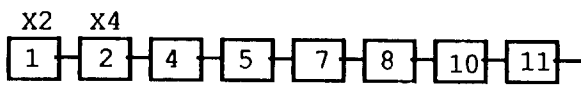

WITH REDUNDANCY

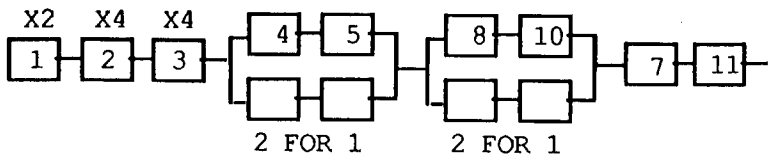

FIGURE 7

WSA/SMA/LSA FORWARD LINK RELIABILITY MODEL

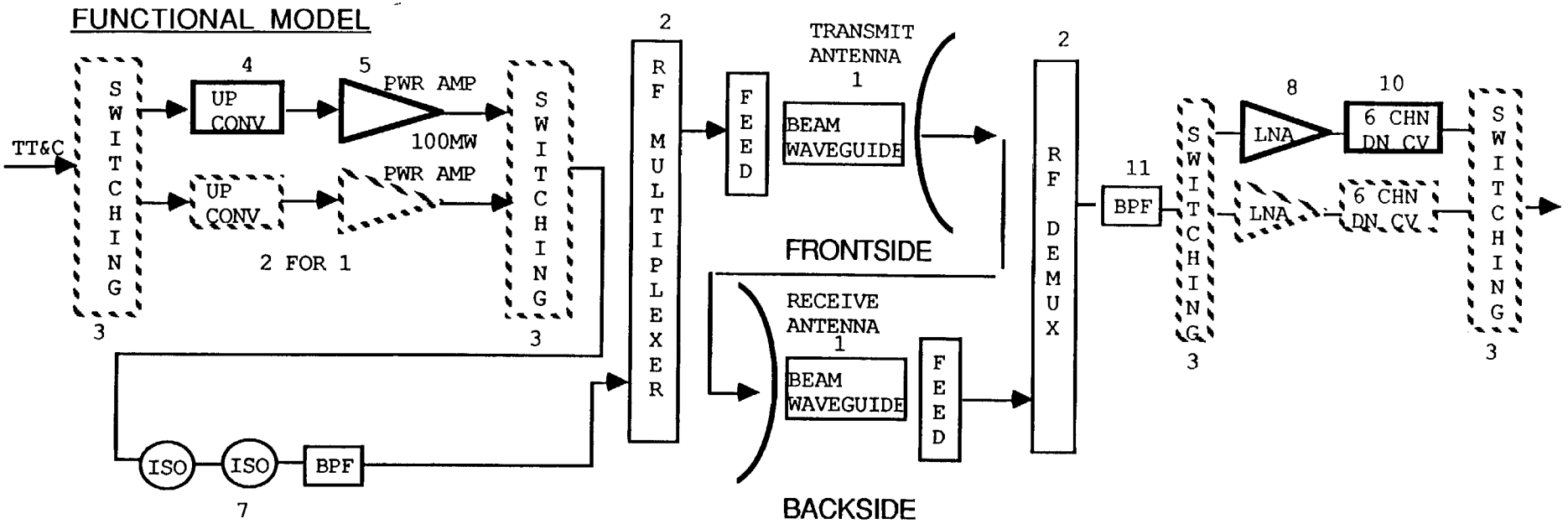

RELIABILITY MODEL

	F.R.
1. ANTENNA/BEAM WG/ FEED	28.5
2. MULTIPLEXER PORT	10
3. SWITCH PORT	5
4. UP CONVERTER	1355
5. 100MW PWR AMP	515
7. BPF/ISOLATOR(2)	15
8. LNA	150
10. DOWN CONVERTER(6 CHN)	1450
11. BPF	5

NO REDUNDANCY

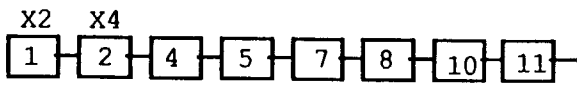

WITH REDUNDANCY

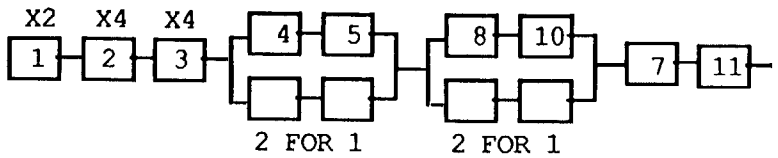

FIGURE 8

TT&C FORWARD LINK RELIABILITY MODEL

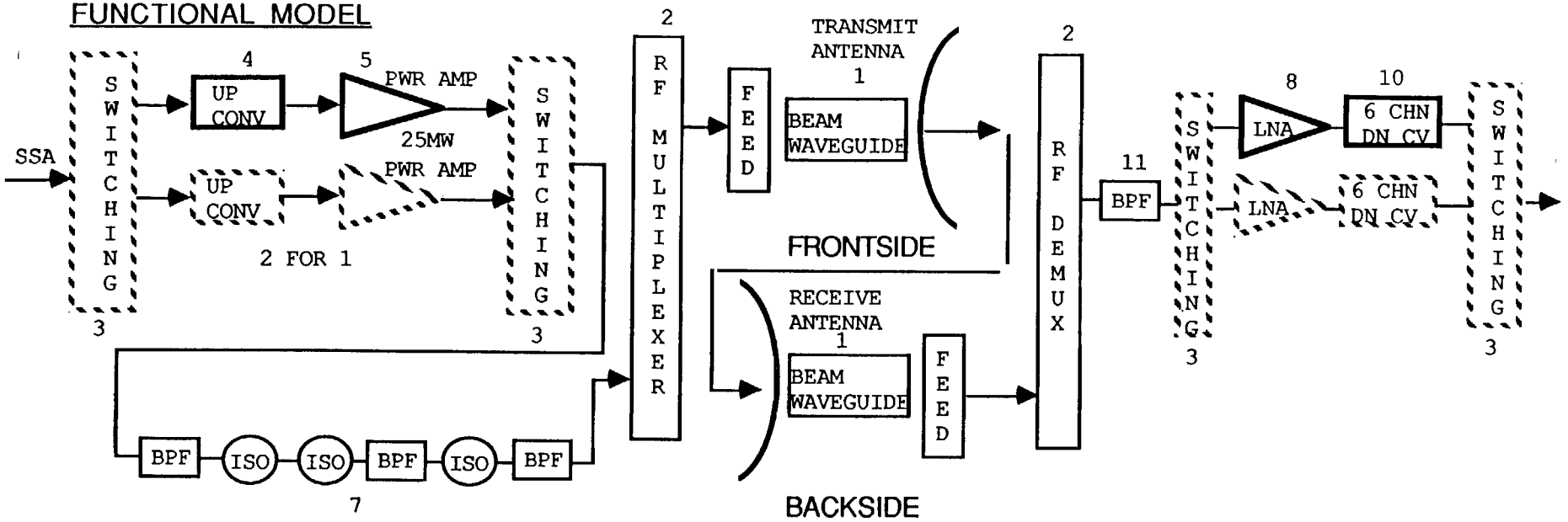

RELIABILITY MODEL

	F.R.
1. ANTENNA/BEAM WG/ FEED	28.5
2. MULTIPLEXER PORT	10
3. SWITCH PORT	5
4. UP CONVERTER	1355
5. 25MW PWR AMP	515
7. BPF(3)/ISOLATOR(3)	30
8. LNA	150
10. DOWN CONVERTER(6 CHN)	1450
11. BPF	5

NO REDUNDANCY

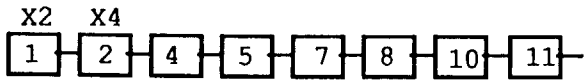

WITH REDUNDANCY

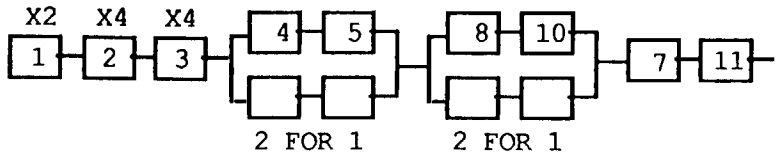

FIGURE 9

SSA FORWARD LINK RELIABILITY MODEL

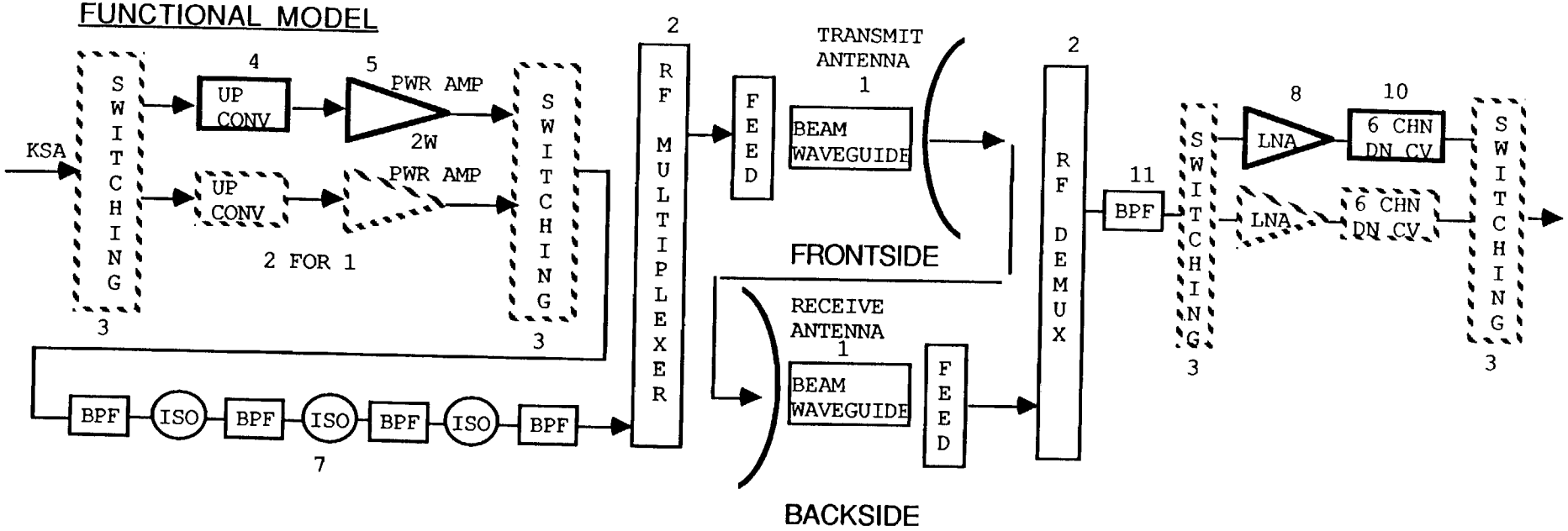

RELIABILITY MODEL

	F.R.
1. ANTENNA/BEAM/WG/ FEED	28.5
2. MULTIPLEXER PORT	10
3. SWITCH PORT	5
4. UP CONVERTER	1355
5. 2W PWR AMP	1515
7. BPF(4)/ISOLATOR(3)	35
8. LNA	150
10. DOWN CONVERTER(6 CHN)	1450
11. BPF	5

NO REDUNDANCY

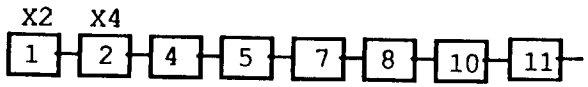

WITH REDUNDANCY

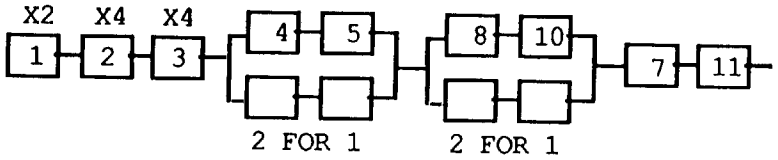

FIGURE 10

KSA FORWARD LINK RELIABILITY MODEL

FUNCTIONAL MODEL

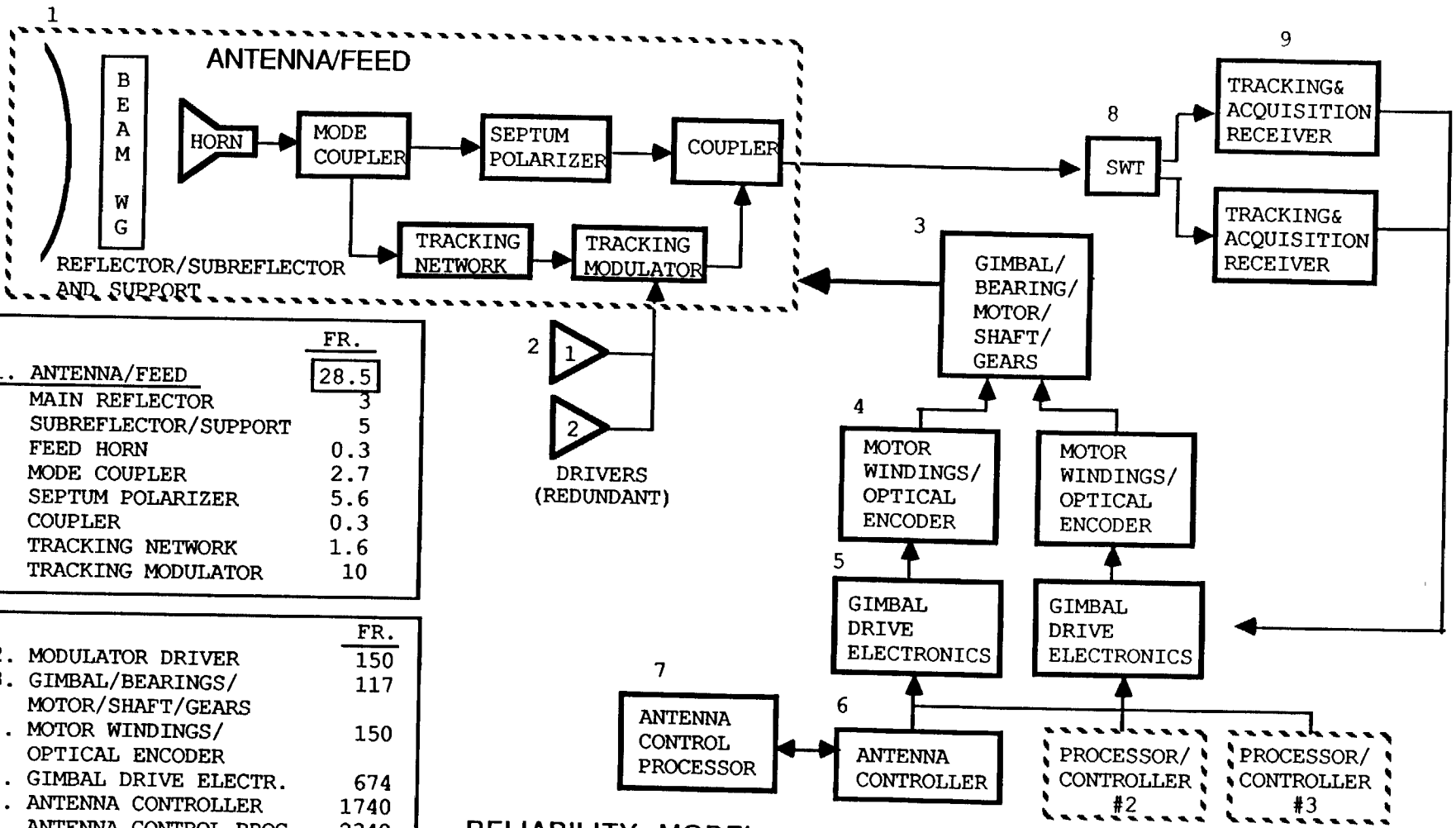

	FR.
1. ANTENNA/FEED	28.5
MAIN REFLECTOR	3
SUBREFLECTOR/SUPPORT	5
FEED HORN	0.3
MODE COUPLER	2.7
SEPTUM POLARIZER	5.6
COUPLER	0.3
TRACKING NETWORK	1.6
TRACKING MODULATOR	10

	FR.
2. MODULATOR DRIVER	150
3. GIMBAL/BEARINGS/ MOTOR/SHAFT/GEARS	117
4. MOTOR WINDINGS/ OPTICAL ENCODER	150
5. GIMBAL DRIVE ELECTR.	674
6. ANTENNA CONTROLLER	1740
7. ANTENNA CONTROL PROC.	2340
8. SWITCH PORT	10
9. TRACKING ACQ. RECEIVER	1721

NOTE; ANTENNA/FEED ITEMS ARE INCLUDED IN THE RETURN AND FORWARD LINK RELIABILITY MODELS.

RELIABILITY MODEL

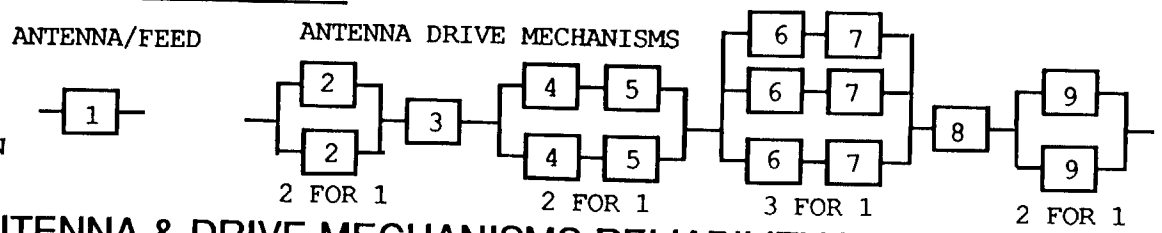

ANTENNA & DRIVE MECHANISMS RELIABILITY MODEL

FIGURE 11